# Lanthanides

**Chapter** · January 2013

CITATION
1

READS
2,540

**1 author:**

Jean-Claude G Bünzli
Hong Kong Baptist University
**525** PUBLICATIONS **23,142** CITATIONS

SEE PROFILE

# LANTHANIDES

## 1. Introduction

Lanthanide elements (Ln: La-Lu; 57–71) belong to the rare-earth series of elements (Sc, Y, and Ln). They present specific chemical, optical, and magnetic properties that are a consequence of their peculiar electronic structure. Although used in small quantities (about 120,000 tons equivalent rare-earth oxides per year worldwide), they have become essential to almost all aspects of modern life, being the active cores in catalysts for oil cracking, lighting devices, high coercivity magnets used in motorization (electric cars, wind turbines, hard disk drives) or audio applications, lasers and telecommunications, biomedical analyses and imaging, and agriculture. They are classified as strategic materials by the military and several governments. This article describes the resources, mining, processing, commercial aspects, physical and chemical properties, as well as all aspects of applications of these elements and their compounds.

## 2. Definition and Discovery

The rare-earth elements (REEs) are a homogeneous group of 17 elements. According to IUPAC nomenclature rules, they correspond to elements 21 (Sc), 39 (Y), and 57–71 (Ln = La-Lu). The latter subgroup should be called "lanthanoids," but "lanthanides" (Ce-Lu) is still the most used designation for metallic elements 57–71 and their compounds (Fig. 1), while rare earths is sometimes used as a synonym for lanthanoids/lanthanides (which will be done here). When it comes to subdividing the lanthanides, there is great confusion. Chemists have the tendency to rely on the electronic structure of the trivalent ions $Ln^{III}$: The light lanthanides (LREEs) are those that have no paired 4f electrons (La-Gd), whereas heavy lanthanides (HREEs) correspond to Dy-Lu. Geochemists use slightly different denominations in that they exclude Eu, which has "anomalous" properties, from the light lanthanides, leaving it alone in a special group; sometimes, a group of middle lanthanides (MREEs) is defined, from Nd to Tb. In metallurgy and industry, LREEs correspond to La-Nd (also called ceric rare earths), MREEs either to Sm-Gd or to Sm-Dy, and HREEs to Dy-Lu or Ho-Lu; finally yttric rare earths are those from Sm to Lu, plus Y. Fortunately, everybody agrees on the nonlanthanoid elements: Yttrium has chemical properties very similar to Dy-Ho, so it is included in HREE, whereas scandium has geochemical and chemical behaviors so different from of all the other REEs that it is not listed in any of these groups. Because of their electropositive nature, rare earths do not appear as elements in nature but, rather, under their oxidized form in salts and minerals. The rare-earth content of minerals, as well as statistics about the extraction, separation, resources, and uses of REE, are always expressed in terms of oxides (rare earth oxide [REO]). The name "earths" also refers to oxides that take the name of the element with the terminal "um" replaced with "a": yttria [1314-36-9] is yttrium oxide $Y_2O_3$, and so on.

The first rare-earth element, yttrium (in fact yttria), has been isolated by the Finnish chemist Johan Gadolin in 1794 from a mineral now named gadolinite and discovered near Ytterby (Sweden). It took more than 100 years (1803–1907) to identify the remaining naturally occurring elements from minerals in which they

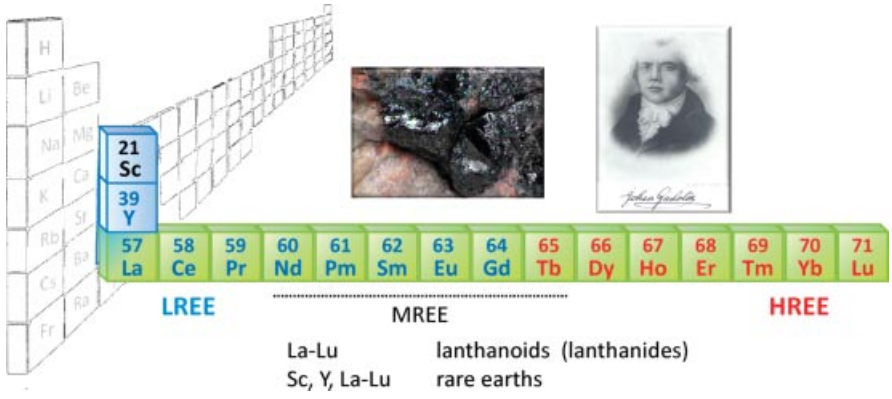


**Fig. 1.** Position of the lanthanoids (lanthanides) and rare earths in the Periodic Table with picture of the black stone of Ytterby from which yttrium oxide was isolated and the portrait of Johan Gadolin. See text for definitions of LREE, HREE, and MREE.

appear as entangled mixtures, whereas radioactive Pm was synthesized in 1947. The thrilling story of the isolation of rare-earth elements is full of incorrect claims and heated disputes among would-be discoverers while reflecting the developments in separation, analytical, and spectroscopic techniques that took place during this span of time. Industrial uses started in 1891 with Carl Auer von Welsbach producing incandescent mantles for gas lighting made up of thorium and cerium oxides and 12 years later the "mischmetall," a mixture of La, Ce, Pr, and Nd to which iron is usually added, for manufacturing flint stones.

## 3. Occurrences of Rare-Earth Elements

Rare-earth elements are distributed broadly in the Earth's crust in relatively small concentrations (10–300 ppm) and always as mixtures. They are found in basalts, granites, gneisses, shales, clays, and silicate rocks. The natural abundances in the Earth's crust and in oceans are listed in Table 2, along with the major isotopes, the atomic radii, and the ground-state electronic configurations. The natural abundances follow the Oddo-Harkins rule, or odd-even effect, such that elements with even-atomic numbers have greater concentrations than the adjacent odd-atomic number elements. The most abundant element in the Earth's crust is clearly cerium (60–68 ppm), followed by neodymium and lanthanum with abundances half that of cerium; praseodymium, samarium, gadolinium, and dysprosium have abundances in the range 5–10 ppm, while other elements are less abundant, with lutetium being the least abundant ($<$0.5 ppm). For a more detailed analysis in different reservoirs, the reader is referred to the article by McLennan and Taylor (1). It is noteworthy that the relative abundances of REE in rock deposits are powerful tools for the study of the formation of these deposits. Neutron-rich lanthanide isotopes occur in the fission of uranium or plutonium and are separated during the reprocessing of nuclear fuel wastes. Otherwise, lanthanide isotopes can be produced by neutron bombardment, by radioactive decay of neighboring atoms, and by nuclear reactions in accelerators where the rare earths are bombarded with charged particles.

Table 1. **Chronology of the Discovery of the Rare-Earth Elements (Data from J. Emsley, *The Elements*, Oxford University Press, Oxford, U.K., 1989)**

| Symb. | At. Nr. | Name | Year | Discoverer(s), place(s) of discovery, origin of name |
|---|---|---|---|---|
| Y | 39 | yttrium | 1794 | J. Gadolin, Åbo, Sweden (Today Turku, Finland). From Ytterby. |
| Ce | 58 | cerium | 1803 | J. J. Berzelius and W. Hisinger, Vestmanland, Sweden. From asteroid Ceres, discovered in 1801 |
| La | 57 | lanthanum | 1839 | C. G. Mosander, Stockholm, Sweden. From *lanthanein*, "hidden" in Greek. |
| Er | 68 | erbium | 1842 | C. G. Mosander, Stockholm, Sweden. From Ytterby. |
| Tb | 65 | terbium | 1843 | C. G. Mosander, Stockholm, Sweden. From Ytterby. |
| Yb | 70 | ytterbium | 1878 | J. C. Galissard de Marignac, Geneva, Switzerland. From Ytterby. |
| Sc | 21 | scandium | 1879 | L. F. Nilson, Uppsala, Sweden. From *Scandia*, Latin word for Scandinavia. |
| Ho | 67 | holmium | 1879 | P. T. Cleve, Uppsala, Sweden; J.-L. Soret and M. Delafontaine, Geneva, Switzerland. From *Holmia*, Latin word for Stockholm. |
| Sm | 62 | samarium | 1879 | P. E. LeCoq de Boisbaudran, Paris, France. From samarskite mineral, found near Samarkand (Uzbekistan). |
| Gd | 64 | gadolinium | 1880 | J. C. Galissard de Marignac, Geneva, Switzerland. In honor of Johan Gadolin. |
| Pr | 59 | praseodymium | 1885 | C. Auer von Welsbach, Vienna, Austria. From Greek words *prasios* (green) and *didymos* (twin). |
| Nd | 60 | neodymium | 1885 | C. Auer von Welsbach, Vienna, Austria. From Greek words *neos* (new) and *didymos* (twin). |
| Dy | 66 | dysprosium | 1886 | P. E. LeCoq de Boisbaudran, Paris, France. From Greek word *dysprositos*, "difficult to access." |
| Eu | 63 | europium | 1901 | E. A. Demarçay, Paris, France. From Europe. |
| Lu | 71 | lutetium | 1907 | G. Urbain, Paris, France. From *Lutetia*, Latin word for Paris. |
| Pm | 61 | promethium | 1947 | J. A. Marinsky, L. E. Glendenin, C. D. Coryell, Oak Ridge, Tenn. From *Prometheus* who stole fire from the gods to give it to mankind. |

Table 2. **Natural Abundances, Principal Isotopes, Electronic Configuration, and Color of the Oxides of Lanthanide Elements**

| Symb. | Abund., ppm[a] | Abund., ng·L$^{-1}$[b] | Principal isotopes, % | | Electronic configuration | Color of oxides[c] |
|---|---|---|---|---|---|---|
| La | 39 | 3.4 | $^{139}$La, 99.91 | | [Xe]4f$^0$5d$^1$6s$^2$ | white |
| Ce | 66.5 | 1.2 | $^{140}$Ce, 88.45 | $^{142}$Ce, 11.11 | [Xe]4f$^1$5d$^1$6s$^2$ | pale yellow |
| Pr | 9.2 | 0.64 | $^{141}$Pr, 100 | | [Xe]4f$^3$6s$^2$ | black |
| Nd | 41.5 | 2.8 | $^{142}$Nd, 27.15 | $^{144}$Nd, 23.80 | [Xe]4f$^4$6s$^2$ | grayish blue |
| Pm | ≈0 | ≈0 | - | | [Xe]4f$^5$6s$^2$ | n.a. |
| Sm | 7.1 | 0.45 | $^{152}$Sm, 26.74 | $^{154}$Sm, 22.73 | [Xe]4f$^6$6s$^2$ | cream |
| Eu | 2.0 | 0.13 | $^{151}$Eu, 47.81 | $^{153}$Eu, 52.19 | [Xe]4f$^7$6s$^2$ | white |
| Gd | 6.2 | 0.7 | $^{158}$Gd, 24.84 | $^{160}$Gd, 21.86 | [Xe]4f$^7$5d$^1$6s$^2$ | white |
| Tb | 1.2 | 0.14 | $^{159}$Tb, 100 | | [Xe]4f$^9$6s$^2$ | brown |
| Dy | 5.2 | 0.91 | $^{164}$Dy, 28.26 | $^{162}$Dy, 25.48 | [Xe]4f$^{10}$6s$^2$ | yellowish |
| Ho | 1.3 | 0.22 | $^{165}$Ho, 100 | | [Xe]4f$^{11}$6s$^2$ | yellowish |
| Er | 3.5 | 0.87 | $^{166}$Er, 33.50 | $^{168}$Er, 26.98 | [Xe]4f$^{12}$6s$^2$ | pink |
| Tm | 0.5 | 0.17 | $^{169}$Tm, 100 | | [Xe]4f$^{13}$6s$^2$ | greenish |
| Yb | 3.2 | 0.82 | $^{174}$Yb, 31.83 | $^{172}$Yb, 21.83 | [Xe]4f$^{14}$6s$^2$ | greenish |
| Lu | 0.8 | 0.15 | $^{175}$Lu, 97.41 | | [Xe]4f$^{14}$5d$^1$6s$^2$ | white |

[a]Abundances in earth crust; values vary depending on sources; data from *Handbook of Chemistry and Physics*, CRC Press, Boca Raton, Fla., 2007.
[b]Abundances in sea water, same source as above.
[c]$Ln_2O_3$, except for Ce ($CeO_2$), Pr ($Pr_6O_{11}$), and Tb ($Tb_4O_7$); most colors are faint.

## 4. Resources and Mining

Currently, more than 100 minerals containing rare earths are known, but only a few are exploited commercially. Most of these minerals are rare in the sense that they are mixed with other minerals so that the highest REO content of currently exploited mines is in the range of 6–10% only. In autumn 2010, China, which was by far the largest rare-earth producer at that time (>95% of the world's production), decided to reduce severely the exportation quotas introduced in 2006, on the grounds of geopolitical and environmental considerations, as well as of a large increase in domestic consumption. This action sent prices of rare earth to a record high, some of them increasing by factors of 10–30, and resulted in the reopening of the U.S.-based Mountain Pass operations in 2012 (project Phoenix; the mine was closed in 2002 because of thorium spill), and starting exploitation of the Australian-based Mount Weld resource the same year. It also stirred a lot of efforts to find new resources and to initiate new mining operations. At the time of this writing, there are 50 rare-earth mineral resources being evaluated in 14 different countries in addition to those in China and India. Japanese geologists have recently proposed to mine deep ocean sediments for rare earths and other rare elements. In 2013, prices are back to more reasonable levels, but cut-off concentrations for ores containing high HREE content can be as low as 0.4% REO. In fact, five elements that are used in phosphors and magnets have been identified as being critical (ie, demand is expected to be larger than production by 2015–2018), yttrium, neodymium, europium, terbium, and dysprosium–four of them belonging to heavy rare earths. Regarding the latter, the main sources have usually low REO content: ion-adsorption clays (<0.5%), eudialyte (0.5–1.5%), xenotime (1–2%), and uranium tailings (5%, but availability is very limited).

Table 3. **Principal Minerals Currently Exploited in the Production of Rare Earths**

| Mineral | Chemical formula | Weight% REO |
|---|---|---|
| | *Cerium group (LREE)* | |
| bastnäsite | $Ln(CO_3)F$ | 65–70 |
| monazite | $LnPO_4$ | 50–75 |
| cerite | $(Ce,La,Ca)_9M^{II}Si_6O_{27}H_4$ | 50–70 |
| loparite-Ce | $(Ce,Na,Ca(Ti,Nb)O_3$ | 31–33 |
| | *Yttrium group (HREE)* | |
| xenotime | $(Y:Ln)PO_4$ | 55–65 |
| gadolinite | $Ln_2FeBe_2Si_2O_{10}$ | 35–50 |
| euxenite | $Ln(Nb,Ta)TiO_6 \times H_2O$ | 15–35 |

The main minerals that are being currently exploited are listed in Table 3 and pictured in Figure 2, whereas the average compositions are given in Table 4. A major problem faced by these mining and subsequent refining operations is the presence of radioactive thorium (4–8% in monazite and 0.1–0.2% in bastnäsite) and uranium (0.1–0.3% in some monazites). In addition, mining, separation, and refining generate large amounts of toxic wastes, gases containing dust concentrates, hydrofluoric and sulfuric acids, and sulfur dioxide, as well as acidic and radioactive wastewater. Costly clean-up operations are under way in China and Malaysia.

A limited number of rare-earth minerals is exploited in large-scale operations. The world's resources are primarily contained in bastnäsite (China and the United States) and monazite (Australia, Brazil, China, India, Malaysia, South Africa, Sri Lanka, Thailand, and the United States); most of the remaining sources are from apatite, cheralite, clay, eudialyte, loparite, phosphorite, and xenotime.

Large deposits of the fluorocarbonate mineral bastnäsite are found in China and near Mountain Pass in California. They constitute the largest share of the world's rare-earth economic sources. Currently, the world's largest deposit of rare earths is located in Bayan Obo, near Baotou in Inner Mongolia, China,

**Fig. 2.** Pictures of the currently exploited rare-earth minerals (from Wikipedia). Top row, cerium group, from left to right: bastnäsite, monazite, cerite, and loparite-Ce; bottom row, yttrium group, from left to right: xenotime, gadolinite, and euxenite.

where bastnäsite is a by-product of iron ore mining. Until recently, it has been estimated that this deposit contains 35 Mt of rare-earth oxides; it now accounts for more than 50% of the Chinese REO production.

Apart from the Mount Weld resource in Australia, monazite is a by-product of titanium ore mining in Australia, Brazil, India, Korea, Malaysia, Thailand, South Africa, and the United States. Deposits of placer sands are dredged and subjected to gravimetric and magnetic separations to isolate ilmenite ($FeTiO_3$, [12168-52-4]), rutile, zircon, monazite, and xenotime. The content of rare-earth minerals in the sands is usually very low (<1%, average 0.1%) compared with the ilmenite content (10%) so that the availability of monazite greatly depends on the world's demand for ilmenite.

Ion-adsorption clay deposits result from prolonged *in situ* weathering of REO-rich rocks, most commonly granitic or volcanic rocks. Critical requirements for the formation of such deposits are met in Southern China, for instance, in the Jiangxi province. A distinctive feature of the REE distribution in these clays is cerium deficiency (see Table 4). The clays are of much lower grade than conventional minerals, but this is compensated by their easy mining and processing. The ore is mined by open-pit methods and leached by dilute aqueous salt solution, which transfers 90% of the rare earths in solution. Rare earths are then precipitated as oxalates or carbonates and converted into mixed REO for separation purposes.

Apatite and other phosphorites constitute an alternative source of rare earths with REO content varying from trace amounts to up to 1%. Apatites richest in REO are found in the Kola Peninsula and in South Africa. Despite

Table 4. **Ln and Y Distribution in Common Mineral Sources (wt% with Respect to 100% REO)**[a]

| | | Regular ores[b] | | | | | Ionic ores[b] | | |
|---|---|---|---|---|---|---|---|---|---|
| Ln | m/W | b/U | b/C | x/M | l/R | NK | Kola | Xun | Long |
| La | 26 | 33.8 | 23 | 1.2 | 28 | 10 | 25.2 | 30 | 2.2 |
| Ce | 51 | 49.6 | 50 | 3.1 | 57.5 | 22.5 | 46.3 | 7.0 | 1.0 |
| Pr | 4 | 4.3 | 6.2 | 0.5 | 3.8 | 2.9 | 3.9 | 7.5 | 1.0 |
| Nd | 15 | 11.2 | 18.5 | 1.6 | 8.8 | 11.3 | 14.2 | 30 | 3.5 |
| Sm | 1.8 | 0.9 | 0.8 | 1.1 | *t* | 3.0 | 1.7 | 6.0 | 2.3 |
| Eu | 0.4 | 0.1 | 0.2 | *t* | 0.1 | 0.4 | 0.53 | 0.5 | 0.2 |
| Gd | 1.0 | 0.2 | 0.7 | 3.5 | *t* | 3.2 | 1.6 | 4.0 | 6.0 |
| Tb | 0.1 | 0.01 | 0.1 | 0.9 | 0.1 | 0.6 | 0.12 | 0.4 | 1.1 |
| Dy | 0.2 | 0.03 | 0.1 | 8.3 | 0.1 | 4.3 | 1.15 | 2.0 | 7.5 |
| Ho | 0.1 | 0.01 | *t* | 2.0 | *t* | 0.9 | 0.11 | 0.4 | 1.7 |
| Er | 0.2 | 0.01 | *t* | 6.4 | *t* | 2.9 | 0.15 | 1.0 | 4.5 |
| Tm | *t* | 0.01 | *t* | 1.1 | *t* | 0.4 | 0.02 | 0.3 | 1.0 |
| Yb | 0.1 | 0.01 | *t* | 6.8 | *t* | 2.7 | 0.08 | 0.06 | 3.5 |
| Lu | *t* | <0.01 | *t* | 1.0 | *t* | 0.4 | 0.01 | 0.3 | 0.5 |
| Y | *t* | 0.1 | *t* | 61 | *t* | 34.6 | 4.9 | 10 | 64 |

[a]Data vary somewhat depending on sources; values do not always sum up to 100% because of rounding and elements in traces.

[b]Key: m/W = monazite from Mount Weld (Australia); b/U = bastnäsite from Mountain Pass (Calif.); b/C ~~monazite from Baotǫ~~ (P.R. China); x/M = xenotime from Malaysia; l/R = loparite from Lovozerskaya (Russia); NK = Norra Kärr mine in Sweden (eudialyte, catapleiite) foreseen to start operations in 2016; Kola = Kola peninsula; Xun = laterite from Xunwu; Long = laterite from Longnam; *t* = traces (<0.1%).

their low REO content, they could become a valuable source of rare earths because they are processed in large quantities for manufacturing fertilizers.

A large deposit of loparite has been found in the Kola Peninsula with ore containing about 2.5% of it, translating to 0.85% REO. Production started in 1951 at the Karnasurt mine in Lovozero Mountain and in 1984 at the Umbozero mine. Output reached a peak between 1988 and 1992 with about 8000 tons of REO per annum produced, but it was progressively reduced to reach current values of about 1700 tons per year. Loparite contains over 30% of REO of the cerium group but has a large concentration of thorium (0.6%) in addition to 0.03% of uranium. In light of the current geopolitical situation, Russia announced at the beginning of 2013 a plan for rejuvenating the Kola Peninsula rare-earth operations and for exploiting the Tomtor Nb/REE deposit in Northern Siberia by 2017.

Like monazite, xenotime is a rare-earth phosphate, but it contains a large amount of yttria (61%) and a greater proportion of HREE. There are two main sources of xenotime, placer sand deposits (where it comes with monazite) and cassiterite ($SnO_2$) ore.

Commercial mining of rare earths started in the late 1890s, and monazite was the major rare-earth ore until 1965. Thereafter, bastnäsite production took over, and it is still the case today. Estimates of the world's production and "industrial" reserves (ie, immediately commercially exploitable) are provided in Table 5. Whereas numbers for production (130 → 110,000 t/years in 2010 → 2012) seem to be reasonably reliable, data for industrial reserves vary wildly according to the definition used and geopolitical interferences. For instance, the U.S. Geological Survey credits China with 55 Mt of industrial reserves in 2012 and 2011, whereas this amount was 36 Mt in 2010, 27 Mt in 2009, and 43 Mt in 2002. The latter figure was still adopted by Chinese officials in 2010, but in 2012, they pretended to have only 23% of the world's industrial reserves. The demand for REO is predicted to increase by about 10% each year during the next 5 years, to reach approximately 180,000 tons in 2017.

The market value of the REO produced is equally difficult to determine with precision in light of the wild variations in prices that have occurred during the past 3 years. Estimates for 2009, 2010, 2011, and 2012 are $1, $2–3, $10–15, and $4–6 billion U.S. These compounds enter in end products with a commercial value of several trillion U.S. dollars, pointing to their special role in industry:

Table 5. **Estimated Mining Production and Industrial Reserves of Rare Earths in 2012. Data from US Geological Survey (Mineral Commodity Summaries, January 2013)**[a]

| Country | Production/t | Reserves/t |
|---|---|---|
| China[b] | 95,000 | 55,000,000 |
| United States | 7,000 | 13,000,000 |
| Australia | 4,000 | 1,600,000 |
| India | 2,800 | 3,100,000 |
| Malaysia | 350 | 30,000 |
| Brazil | 300 | 36,000 |
| other countries | n.a. | 41,000,000 |
| *Total* | *110,000* | *110,000,000* |

[a]Official data from Russia are not available (estimated present production 1700 tons/year; industrial reserves 19,000,000 T – included in ROW figure).
[b]See text.

indispensable but often in minute quantities. As a typical example, a smartphone contains about 150–250 mg of nine different rare earths' worth between $1 and $2.

## 5. Basic Properties of Lanthanide Elements

For commodity, the elements Ce-Lu are listed separately in the Periodic Table (2), although it is usually assumed that they belong to Group 3, which encompasses Sc, Y, La, and Ac. These elements have electronic configurations $nd^1(n+1)s^2$, and they introduce the d transition elements series: 3d (Sc), 4d (Y), 5d (La), and 6d (Ac). It happens that the energy of the 4f atomic orbitals decreases abruptly beyond La, so that the 4f electron shell fills; the electronic configurations of the lanthanides are listed in Table 2, whereas selected physical properties are reported in Table 6 and Table 7. Gschneidner and Daane (3) gave a comprehensive account of the preparation, metallurgy, solid-state physics, and chemical properties of the rare-earth metals. These metals form alloys with most other metals and can be present interstitially in solid solutions or as intermetallic compounds in secondary phases. Alloying with other elements can render rare earths either pyrophoric, as in the "mischmetall," or corrosion resistant. When determining physical constants, it is extremely important that the materials are highly pure and well characterized. Ames Laboratory (Ames, Iowa) has been a leader in this field, preparing the first rare-earth metals with a purity of 99.99% with respect to all elements.

The large electropositive nature of the rare-earth elements precludes obtaining metals by reduction of oxides or salts with carbon. There are two methods of preparations for metals. The first one is the electrolysis of fused oxides or salts in the presence of an $LnF_3$ flux; this can only be done for elements La through Nd because the melting points of the medium and heavier elements are too high. "Mischmetall" is commonly produced in this way either from a fused chloride or a fluoride bath. Alternatively, rare-earth metals can be electrodeposited with a solvent metal (Zn or Mg) and subsequently distilled from the mixture. The selection of materials for the electrolysis cell is difficult because of the high reactivity of the rare-earth metals. The containment crucible is typically built from molybdenum, tungsten, tantalum, or sometimes iron with a ceramic or graphite lining. The cathode is usually molybdenum or a soluble transition metal (to produce a eutectic); the anode is frequently carbon.

The second method relies on metallothermal reduction and can be applied to all lanthanide metals and yttrium. Suitable reducing agents are alkali metals, alkaline-earth metals, aluminum, or light lanthanide metals prepared by electrolysis. A preferred process, calciometric reduction, uses the redox properties of calcium and works for rare earths with melting points larger than 1050°C (Y, Gd, Tb, Dy, Ho, Er, and Lu); it proceeds in a tantalum crucible according to the following reactions:

$$\begin{aligned} Ln_2O_3 &+ 3(NH_4F\cdot HF) \xrightarrow{700^\circ C} 2LnF_3 + 3H_2O + 3\,NH_3 \\ 2LnF_3 &+ 3Ca \xrightarrow{1500^\circ C} 2Ln + 3\,CaF_2 \end{aligned} \qquad (1)$$

Alternatively, ammonium fluoride can be replaced with hydrochloric acid, which leads to lower reaction temperatures (600°C and 1200°C). Another example is lanthanometric reduction based on the reduction of $Ln_2O_3$ oxides (Ln = Sm,

Table 6. **Physical Properties of Lanthanide Elements La-Eu**

| Parameter | La | Ce | Pr | Nd | Pm | Sm | Eu |
|---|---|---|---|---|---|---|---|
| CAS number | [7439-91-0] | [7440-45-1] | [7440-10-0] | [7440-00-8] | [7440-12-2] | [7440-19-9] | [7440-53-1 |
| atomic number | 57 | 58 | 59 | 60 | 61 | 62 | 63 |
| atomic weight | 138.91 | 140.12 | 140.908 | 144.24 | (145) | 150.36 | 151.96 |
| melting point °C | 918 | 798 | 931 | 1021 | 1042 | 1074 | 822 |
| boiling point °C | 3464 | 3433 | 3520 | 3074 | ~3000 | 1794 | 1429 |
| density at 25°C in g/cm$^3$ | 6.1453 | 6.770 | 6.773 | 7.007 | 7.22 | 7.520 | 5.234 |
| heat of fusion in kJ/mol | 6.201 | 5.179 | 6.912 | 7.134 | 8.623 | 9.221 | |
| heat of sublimation at 25°C, kJ/mol[b] | 431.0 | 422.6 | 355.6 | 327.6 | ~348 | 206.7 | 144.7 |
| conduction electrons | 3 | 3.1 | 3 | 3 | 3 | 3 | 2 |
| crystal structure | hcp | dhcp | dhcp | dhcp | dhcp | rhomb. | bcc |
| atomic radius in pm[a] | 187.9 | 182.5 | 182.8 | 182.1 | 181.1 | 180.4 | 204.2 |
| Néel point, °C | n.a | ≈13 | n.a | n.a | n.a | 15 | 90 |

[a]rhomb: rhombohedral.
[b]For CN = 12 and the $\alpha$-form at room temperature.

Table 7. **Properties of Lanthanide Elements Gd-Lu**

| Parameter | Gd | Tb | Dy | Ho | Er | Tm | Yb | Lu |
|---|---|---|---|---|---|---|---|---|
| CAS Nr. | [7440-54-2] | [7440-27-9] | [7429-91-6] | [7440-60-0] | [7440-52-0] | [7440-30-4] | [7440-64-4] | [7439-94-3] |
| atomic number | 64 | 65 | 66 | 67 | 68 | 69 | 70 | 71 |
| atomic weight | 157.95 | 158.9254 | 162.50 | 164.930 | 167.26 | 168.934 | 173.04 | 174.97 |
| melting point °C | 1313 | 1365 | 1412 | 1474 | 1529 | 1545 | 819 | 1663 |
| boiling point °C | 3273 | 3230 | 2567 | 2700 | 2868 | 1950 | 1196 | 3402 |
| density at 25°C in g/cm$^3$ | 7.9004 | 8.2294 | 8.5500 | 8.7947 | 9.066 | 9.3208 | 6.9654 | 9.8404 |
| heat of fusion in kJ/mol | 10.05 | 10.80 | 10.782 | 16.874 | 19.90 | 16.84 | 7.657 | 18.65 |
| heat of sublimation at 25°C, kJ/mol | 397.5 | 288.7 | 290.4 | 300.8 | 317.10 | 232.2 | 152.1 | 427.6 |
| conduction electrons | 3 | 3 | 3 | 3 | 3 | 3 | 2 | 3 |
| crystal structure | hcp | hcp | hcp | hcp | hcp | hcp | fcc | hcp |
| atomic radius in pm[a] | 180.1 | 178.33 | 177.43 | 176.61 | 175.66 | 174.62 | 193.92 | 173.49 |
| Curie point, °C | 292.7 | 220 | 86 | 19 | 18 | 32 | n.a. | n.a |
| Néel point, °C | n.a. | 230 | 178 | 133 | 84 | 56 | n.a. | n.a |

[a]For CN = 12 and the $\alpha$-form at room temperature.

Eu, Tm, and Yb) by La or by the "mischmetall." Purification is then achieved by either distillation or sublimation.

Metals crystallize in different close-packed crystal structures, hexagonal closed-packed (hcp), double hexagonal closed-packed (dhcp), body-centered cubic (bcc), face-centered cubic (fcc), or for Sm, a rhombohedral structure. Their atomic radii clearly correspond to those of +3 ions, except for Eu and Yb, which are larger and correspond to +2 ions. The rare-earth metals have a great affinity for oxygen, sulfur, nitrogen, carbon, silicon, boron, phosphorus, and hydrogen at elevated temperature and remove these elements from most other metals, henceforth, their utility in metallurgy.

## 6. Chemical Properties of Lanthanide Ions

All rare-earth elements are highly electropositive with Pauling's electronegativity values between 1.10 and 1.27. Their most stable oxidation state is +3 with electronic configuration $[Xe]4f^n$ ($n = 0$–14), as shown by the redox potentials listed in Table 8 (4). Some elements can, however, be obtained at +2 (Sm, Eu, Yb) or +4 (Ce, Pr, Tb) oxidation states without too much difficulty. In fact, the field of low valence lanthanide compounds has progressed tremendously during the past years with respect to both inorganic compounds (10) and molecular complexes, with currently 11 of the latter fully characterized in organic solvents or solid state (Ln = Y, La, Ce, Nd, Sm, Eu, Dy, Ho, Tm, Er, Yb); moreover, divalent reduction chemistry with organometallic compounds is known for most of the others (11). Some lanthanide monohalides have also been characterized as well as a few $Ln^0$ compounds (11).

Selected characteristics of trivalent lanthanide ions are reported in Table 8. The electronic configurations $[Xe]4f^n$ determine their properties: Because the xenon core contains the $5s^25p^6$-filled subshells, 4f electrons are shielded from external interactions. As a consequence, $Ln^{III}$ ions display similar chemical properties, are hard cations according to Pearson's classification, and are essentially involved in ionic or ion-dipole bonding, with little covalency. The latter is usually less than 5%, and when it is detected, it often stems from contributions from the 5d orbitals. A survey of 1391 crystal structures showed that 42% of the scrutinized complexes contain exclusively Ln-O bonds while 78% contain at least one Ln-O bond (12). The stability of the trivalent state results from the fourth ionization potential being larger than the sum of the first three ionization energies, with the exceptions of Ce, Tb, and Yb. The first two elements, particularly Ce, form +3 and +4 compounds, whereas Yb, which has large third ionization energy, forms +2 compounds instead. In aqueous solution, all trivalent lanthanides are very stable, whereas only $Ce^{IV}$ and $Eu^{II}$ exist. The properties of these cations are very different from those of the trivalent lanthanides. For example, $Ce^{IV}$ is more acidic and $Ce^{IV}$ hydroxide precipitates at pH 1; $Eu^{II}$ is less acidic and $Eu^{II}$ hydroxide does not precipitate in the pH range 6–8, whereas trivalent lanthanide hydroxides do. Some industrial separations are based on these differences.

Lanthanide chlorides, bromides, nitrates, bromates, and perchlorates are soluble in water, and when their aqueous solutions evaporate, they crystallize as hydrated salts. Acetates, iodates, and iodides are somewhat less soluble. Sulfates are sparingly soluble and exhibit a negative solubility trend with

Table 8. **Selected Properties of Trivalent (and Divalent) Lanthanide Ions**[a]

| Ln[b] | $\chi_P$ | $I_1$ | $I_{1-3}$ | $E^0_{r,3-0}$ | $E^0_{r,3-2}$ | $\Delta H^0_{h(III)}$ | $\Delta H^0_{h(II)}$ | $-\log^*\beta 11$ | pH | $r_i(6)$ | $r_i(9)$ | $r_i(12)$ |
|---|---|---|---|---|---|---|---|---|---|---|---|---|
| La | 1.10 | 538 | 3455 | −2.522 | −3.1 | 3326 | n.a. | 9.01 | 7.47 | 1.03 | 1.22 | 1.36 |
| Ce | 1.12 | 1949 | 3523 | −2.483 | −2.92 | 3380 | 1397 | 10.6 | 7.10 | 1.01 | 1.20 | 1.34 |
| Pr | 1.13 | 2086 | 3627 | −2.462 | −2.84 | 3421 | 1309 | 8.55 | 6.96 | 0.99 | 1.18 | 1.32 |
| Nd | 1.14 | 2132 | 3694 | −2.431 | −2.62 | 3454 | 1317 | 8.43 | 6.78 | 0.98 | 1.16 | 1.30 |
| Pm | 1.13 | 2152 | 3738 | −2.423 | −2.44 | 3482 | 1346 | n.a. | n.a. | 0.97 | 1.14 | 1.28 |
| Sm | 1.17 | 2258 | 3871 | −2.414 | −1.50 | 3512 | 1344 | 8.34 | 6.65 | 0.96 | 1.13 | 1.27 |
| Eu | 1.2 | 2404 | 4035 | −2.407 | −0.35 | 3538 | 1361 | 8.31 | 6.61 | 0.95 | 1.12 | 1.25 |
| Gd | 1.20 | 1991 | 3750 | −2.397 | −2.85 | 3567 | 1555 | 8.35 | 6.58 | 0.94 | 1.11 | 1.24 |
| Tb | 1.1 | 2114 | 3790 | −2.391 | −2.83 | 3600 | 1464 | 8.16 | 6.47 | 0.92 | 1.10 | 1.23 |
| Dy | 1.22 | 2200 | 3898 | −2.353 | −2.56 | 3634 | 1437 | 8.10 | 6.24 | 0.91 | 1.08 | 1.22 |
| Ho | 1.23 | 2204 | 3924 | −2.319 | −2.79 | 3663 | 1433 | 8.04 | 6.20 | 0.90 | 1.07 | 1.21 |
| Er | 1.24 | 2194 | 3934 | −2.296 | −2.87 | 3692 | 1453 | 7.99 | 6.14 | 0.89 | 1.06 | 1.19 |
| Tm | 1.25 | 2285 | 4045 | −2.278 | −2.22 | 3717 | 1451 | 7.95 | 5.98 | 0.88 | 1.05 | 1.18 |
| Yb | 1.1 | 2417 | 4194 | −2.267 | −1.15 | 3740 | 1461 | 7.92 | 5.87 | 0.87 | 1.04 | 1.17 |
| Lu | 1.27 | 524 | 3886 | −2.255 | n.a. | 3759 | n.a | 7.90 | 5.74 | 0.86 | 1.03 | 1.16 |

[a]Data are for $Ln^{III}$ ions except $\Delta H^0_{h(II)}$.

[b]Key: $\chi_P$ = Pauling's electronegativity; $I_1$ first ionization energy (rounded to 1 kJ·mol$^{-1}$); $I_{1\text{-}3}$ = sum of the first 3 ionization energies (rounded to 1 kJ·mol$^{-1}$); $E^0_{r,3-0}$ = redox potential $Ln^{+3}/Ln^0$ in V; $E^0_{r,3-2}$ = redox potential $Ln^{+3}/Ln^{+2}$ in V, value for La is calculated (5); $\Delta H^0_h(III)$ = hydration enthalpies for trivalent ions, rounded to 1 kJ·mol$^{-1}$ (6); $\Delta H^0_h(II)$ = hydration enthalpies for divalent ions, rounded to 1 kJ·mol$^{-1}$ (4); $^*\beta_{11} = [(LnOH)^{2+}][H^+]/[Ln^{3+}]$, ionic strength = 0.3 M; data from 7; pH = pH at which precipitation starts in $Ln(NO_3)_3$ solutions 0.1 M in water 8; $r_i(n)$ = ionic radii for coordination numbers $n = 6$, 9, and 12 in Å (9).

increasing temperature. Oxides, sulfides, fluorides, carbonates, oxalates, and phosphates are insoluble in water. Sparingly soluble oxalates are important in the selective recovery of lanthanides from solutions, and this property is used in analytical and industrial applications. Lanthanides readily form double salts, such as $Ln_2(SO_4)_3 \times 3Na_2SO_4 \times 2H_2O$ and $Ln_2(SO_4)_3 \times MgSO_4 \times 24H_2O$, which are used in fractionation processes. Anhydrous rare-earth salts cannot be prepared by evaporating water: For example, when heated, $LnCl_3 \times 6H_2O$ converts partially into the oxychlorides and so do nitrates, which yield oxynitrates. To get anhydrous chloride, the hydrated salts are heated slowly while a stream of anhydrous HCl gas is passed over them. Nitrates may be obtained without crystallization water by careful heating under high vacuum ($10^{-6}$ mmHg). Alternatively, the salts can be mixed with ammonium chloride and sublimation leaves the anhydrous compounds as residue. Finally, many binary anhydrous salts can be prepared by combining the metal directly with an electronegative element; for example, $Cl_2$ over Ln gives $LnCl_3$ and Ln plus S gives $Ln_2S_3$. Lanthanides also form hydrides of any composition up to $LnH_3$, which desorb hydrogen reversibly with temperature. Therefore, some lanthanides and their alloys are used for hydrogen storage (see the End Uses of Rare Earths section). Many binary compounds of the lanthanides, such as oxides, nitrides, and carbides, can exist as nonstoichiometric solids.

Numerous complexes of lanthanides with organic ligands (13) are known. Some of these compounds are water soluble, whereas others are oil soluble. Water-soluble compounds have been used extensively in the past for rare-earth separation by ion exchange; examples are complexes with citric acid, ethylenediaminetetraacetic acid (EDTA), and hydroxyethylethylenediaminetriacetic acid (HEDTA). Oil-soluble compounds are being used extensively in the industrial separation of rare earths by liquid–liquid extraction.

The ionic radii of $Ln^{III}$ ions are large and depend on both the ion and the coordination number (CN). They do not vary much along the series, but the change is gradual and reflects the *lanthanide contraction*. Although coordination numbers between 3 and 12 are well documented (Table 9), most complexes exhibit coordination numbers 8 (37%) or 9 (26%), with CN = 6 (9%), 7 (8%), and 10 (11%) being also well represented (12). Because the geometrical arrangement around the lanthanide ions essentially depends on the steric properties of the ligand, specific coordination numbers are obtained with a suitable design of the ligating molecules. Coordination numbers 3 to 5 occur with bulky ligands, but there are few examples. Coordination number 6 represents a special historical case. Even though the first crystal structure of a lanthanide aqua ion, $[Nd(H_2O)_9](BrO_3)_3$, was determined in 1939 and clearly pointed to nine-coordination, a commonly expressed opinion, influenced by d-transition coordination chemistry, was that the rare-earth ions formed six-coordinate, octahedral complexes. It was the pioneering work of G. Schwarzenbach on polyaminocarboxylate complexes of yttrium and cerium in the early 1960s that casted doubt about this thinking. The six-coordinate theory definitely died in 1965 when Hoard and co-workers published the molecular structures of the lanthanum ethylenediaminetetraacetate complexes $NH_4La(EDTA)\cdot 8H_2O$ and $HLa(EDTA)\cdot 7H_2O$: The latter were found to contain nine- and ten-coordinate $La^{III}$ ions, respectively (29). Nevertheless, six-coordination is found in several lanthanide compounds, of

Table 9. **Observed Coordination Numbers of $Ln^{III}$ Ions in the Solid State, with Typical Examples**

| CN | Idealized geometry | Idealized symmetry | Examples[a] | Ref. |
|---|---|---|---|---|
| 3 | pyramidal | $C_{3v}$ | $[Eu[N(SiMe_3)_2]_3]$ | (14) |
| | | | $[Ln[N(i\text{-}prop)_2]_3]$ | (15) |
| 4 | tetrahedral | $T_d$ | $[Ln[N(i\text{-}prop)_2]_3]^-$ | (15) |
| 5 | trigonal bipyramidal | $D_{3h}$ | $[Tm[P(SiMe_3)_2]_3(THF)_2]$ | (16) |
| 6 | octahedral | $O_h$ | $[Er(NCS)_6]^{3-}$ | (14) |
| | trigonal prism | $D_{3h}$ | $[Er(DPM)_3]$ | (14) |
| 7 | pentagonal bipyramidal | $D_{5h}$ | $[Eu(DPM)_3(DMSO)]$ | (14) |
| | capped octahedron | $C_{3v}$ | $[Ho(DBM)_3(H_2O)]$ | (14) |
| | capped trigonal prism | $C_{2v}$ | $[LaI_3(i\text{-}propOH)_4]$ | (17) |
| 8 | square antiprism | $D_{4d}$ | $[Lu(H_2O)_8]^{3+}$ | (18) |
| | bicapped trigonal prism | $C_{2v}$ | $[LaCl_3(15C5)]$ | (19) |
| | dodecahedron | $C_{2v}$ | $[Tb(TETA)_4]^-$ | (20) |
| 9 | tricapped trigonal prism | $D_{3h}$ | $[Eu(H_2O)_9]^{3+}$, $[Ln(MeCN)_9]^{3+}$, $[Eu(mbzimpy)_3]^{3+}$ | (21–23) |
| | capped square antiprism | $C_{2v}$ | $[Pr\,Cl_3(terpy)(H_2O)_3]$ | (14) |
| 10 | bicapped square antiprism | $D_{4d}$ | $[La(EDTA)(H_2O)_4]^-$ | (14) |
| | $C_{2v}$ dodecahedron | $C_{2v}$ | $[Eu(NO_3)_5]^{2-}$ | (24) |
| | tetracapped hexagon | $D_{2h}$ | $[Nd(NO_3)_2(18C6)]^+$ | (25) |
| 11 | (pentacapped trigonal prism)[b] | $(D_{3h})$[b] | $[La(NO_3)_3(H_2O)_5]$ | (26) |
| | heptadecahedral | $C_S$ | $[Eu(NO_3)_3(15C5)]$ | (27) |
| 12 | icosahedron | $I_h$ | $[Ce(NO_3)_6]^{3-}$ | (14) |
| | distorted icosahedron | $C_1$ | $[Nd(NO_3)_3(18C6)]$ | (28) |

[a]Key: 15C5 = 15-crown-5 ether; 18C6 = 18-crown-6 ether; DBM = dibenzoylmethane; DMSO = dimethylsulfoxide; DPM = dipivaloylmethane; i-prop = isopropyl; mbzimpy = bis(N-methyl-benzimidazole)-pyridine; TETA = 1,4,8, 11-tetraazacyclotetradecane-1,4,8,11-tetraacetic acid; THF = tetrahydrofuran; terpy = terpyridine.

[b]Known 11-coordinated lanthanide complexes deviate strongly from this idealized geometry.

which the most representative are the elpasolites containing $[LnX_6]^{3-}$ hexahalide anions. Other octahedral complexes are also known, for instance, with the $\beta$-diketonate anion of dipivaloylmethane, with hexamethylphosphoramide, or with tetramethylurea. Substantial numbers of lanthanide complexes are known to have coordination numbers 7 through 12, with the more common coordination numbers ranging, however, between 8 and 10 (14).

Complexes with polydentate macrocyclic ligands, coronands, cryptands, calixarenes, and acyclic and cyclic Schiff bases have coordination numbers that often extend to 11 and 12. The coordination polyhedra deviate substantially from the idealized symmetrical structure of lowest energy calculated on the basis of $n$ identical Ln-ligand chemical bonds, and the deviation often increases with the ligand complexity. It is important to realize that for large coordination numbers, the energy of reorganization in going from one polyhedron to another, or even, in solution, in going from one coordination number to the next one by addition of a solvent molecule, is fairly small. Large coordination numbers are also found in some simple inorganic nitrato complexes; compare $La(NO_3)_3(H_2O)_5$ or the hexanitratolanthanate(III) anions with octahedrally arranged bidentate nitrates.

When complexation occurs in water, complex formation has to overcome the large hydration energies of the $Ln^{III}$ ions, so that chelating agents are usually preferred to benefit from a sizeable entropic stabilization; in addition,

Table 10. **Selected Stability Constants of Inner Sphere Complexes with Simple Inorganic Ligands in Water at 295 K and $I = 1.0\ M$ (30)**

| Ln | Fluoride | Sulfate[a] | | Carbonate | | Nitrate |
|---|---|---|---|---|---|---|
| | $\text{Log}\beta_1$ | $\text{Log}\beta_1$ | $\text{Log}\beta_2$ | $\text{Log}\beta_1$ | $\text{Log}\beta_4$ | $\text{Log}\beta_1$ |
| Y | 3.60 | 1.24 | 1.68 | 6.02[b] | n.a. | −0.17[c] |
| La | 2.67 | 1.29 | n.a. | 5.67[b] | 14.45[d] | −0.26 |
| Nd | 3.09 | 1.26 | 1.79 | n.a. | 15.35[d] | +0.02 |
| Eu | 3.19 | 1.37 | 1.96 | 5.88 | 14.3 | +0.20 |
| Tb | 3.42 | 1.27 | 1.89 | n.a. | 16.24[d] | −0.03 |
| Er | 3.54 | 1.23 | 1.71 | n.a. | 16.92[d] | −0.33 |
| Lu | 3.61 | 1.09 | 1.61 | n.a. | 17.07[d] | −0.2 |

[a] $I = 2.0$ M
[b] $I = 3.0$ M
[c] At 293 K, $I = 3.0$ M
[d] $I = 2.5$ M

preorganization of the ligand is also a beneficial factor (eg, the macrocyclic effect). Divalent ions have smaller hydration enthalpies, comparable with that of $Ca^{II}$. Hydrolysis is often a problem when working at basic pH or around neutral pH. Complexation reactions are assumed to follow the Eigen mechanism, involving an initial diffusion-controlled formation of an "outer" sphere intermediate in which the $Ln^{III}$ cation and the (often negatively charged) ligand associate to yield a solvent-separated pair. If a change in coordination number occurs during the complexation reaction, then it is most often coupled with the expulsion of solvent molecules. Stability constants for the complexation of inorganic anions and of organic chelating agents are listed in Table 10 (30) and Figure 3 (30,31), respectively. The chelate effect is clearly seen in going from acetate (1 carboxylate) to malonate (2 carboxylates) and from malonate to EDTA

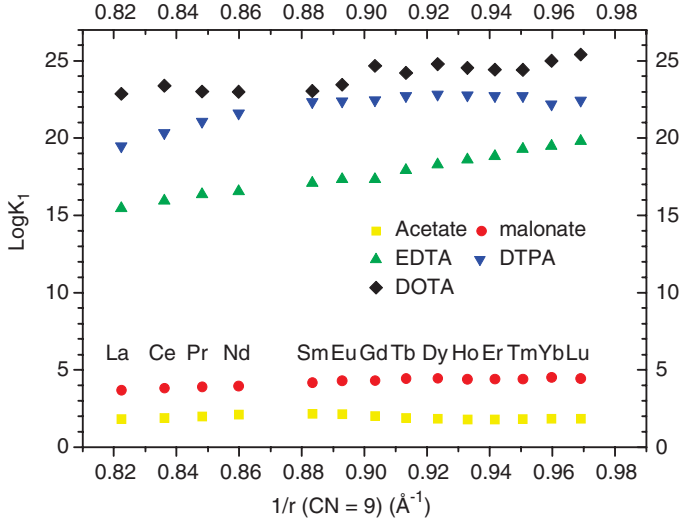


**Fig. 3.** Stability constants in water, at 298 K of lanthanide complexes with several carboxylates (30,31). DTPA = diethylenetriaminepentaacetate (30) and DOTA = 1,4,7,10-tetraazacyclododecane-1,4,7,10-tetraacetatic acid.

(4 carboxylates and 2 amines) and DTPA (5 carboxylates and 3 amines). The macrocyclic effect is evidenced in going from EDTA to DOTA.

Another salient feature of trivalent lanthanide ions in aqueous solution is their high rate of water exchange that decreases from $8.3 \times 10^8\,s^{-1}$ for $Gd^{III}$ to $4.7 \times 10^7\,s^{-1}$ for $Yb^{III}$, while it is estimated to lie in the range $5 \times 10^8$ to $10^9\,s^{-1}$ for the lighter lanthanide ions; the rate is an order of magnitude larger for the $Eu^{II}$ aqua ion, $5 \times 10^9\,s^{-1}$ (32).

## 7. Optical Properties of Lanthanide Ions

The [Xe]$4f^n$ electronic configurations of the $Ln^{III}$ ions generate a wealth of electronic levels (33). In light of the shielding of the 4f electrons, these levels are well defined and both absorption and emission bands are sharp. Moreover, interactions with the ligands are weak, resulting in splitting of electronic levels of a few hundred $cm^{-1}$ only so that electronic properties may be adequately described within the frame of the ligand (crystal) field theory; the Russels–Saunders scheme for spin-orbit coupling is also usually assumed, so that the electronic configurations are characterized by the three quantum numbers $S$, $L$, and $J$. More detailed calculations need, however, to be conducted within the frame of the intermediate spin-orbit coupling scheme. Basic properties are summarized in Table 11, whereas a partial electronic level diagram is given in Figure 4 (34). It is noteworthy that currently this diagram has been experimentally extended up to about $70\,000\,cm^{-1}$, whereas calculations have been performed for levels up to $193{,}000\,cm^{-1}$. The splitting of the electronic levels under ligand field interaction is given in Table 12 and is useful for the determination of the site symmetry of the lanthanide ion either by absorption or by emission spectroscopy.

**7.1. Absorption Spectra.** The absorption of light is achieved through operators related to the nature of electromagnetic waves: the odd-parity electric dipole (ED), the even-parity magnetic dipole (MD), and the electric quadrupole (EQ) operators. Transitions between an initial state $\Psi_i$ and a final state $\Psi_f$ follow specific selection rules that depend on the nature of the operator and of the initial and final states, as well as on the symmetry of the chemical environment of the metal ion. Transitions involving lanthanide ions are of three different kinds.

1. Sharp intraconfigurational 4f–4f transitions featuring rearrangement of the electrons within the $4f^n$ subshell. Electric dipole transitions are

Table 11. **Electronic Properties of $Ln^{III}$ Ions**

| $f^n$ | | Multiplicity | Nr of terms | Nr of levels | Ground level | |
|---|---|---|---|---|---|---|
| $f^0$ | $f^{14}$ | 1 | 1 | 1 | $^1S_0$ | $^1S_0$ |
| $f^1$ | $f^{13}$ | 14 | 1 | 2 | $^2F_{5/2}$ | $^2F_{7/2}$ |
| $f^2$ | $f^{12}$ | 91 | 7 | 13 | $^3H_4$ | $^3H_6$ |
| $f^3$ | $f^{11}$ | 364 | 17 | 41 | $^4I_{9/2}$ | $^4I_{15/2}$ |
| $f^4$ | $f^{10}$ | 1001 | 47 | 107 | $^5I_4$ | $^5I_8$ |
| $f^5$ | $f^9$ | 2002 | 73 | 198 | $^6H_{5/2}$ | $^6H_{15/2}$ |
| $f^6$ | $f^8$ | 3003 | 119 | 295 | $^7F_0$ | $^7F_6$ |
| $f^7$ | | 3432 | 119 | 327 | $^8S_{7/2}$ | |

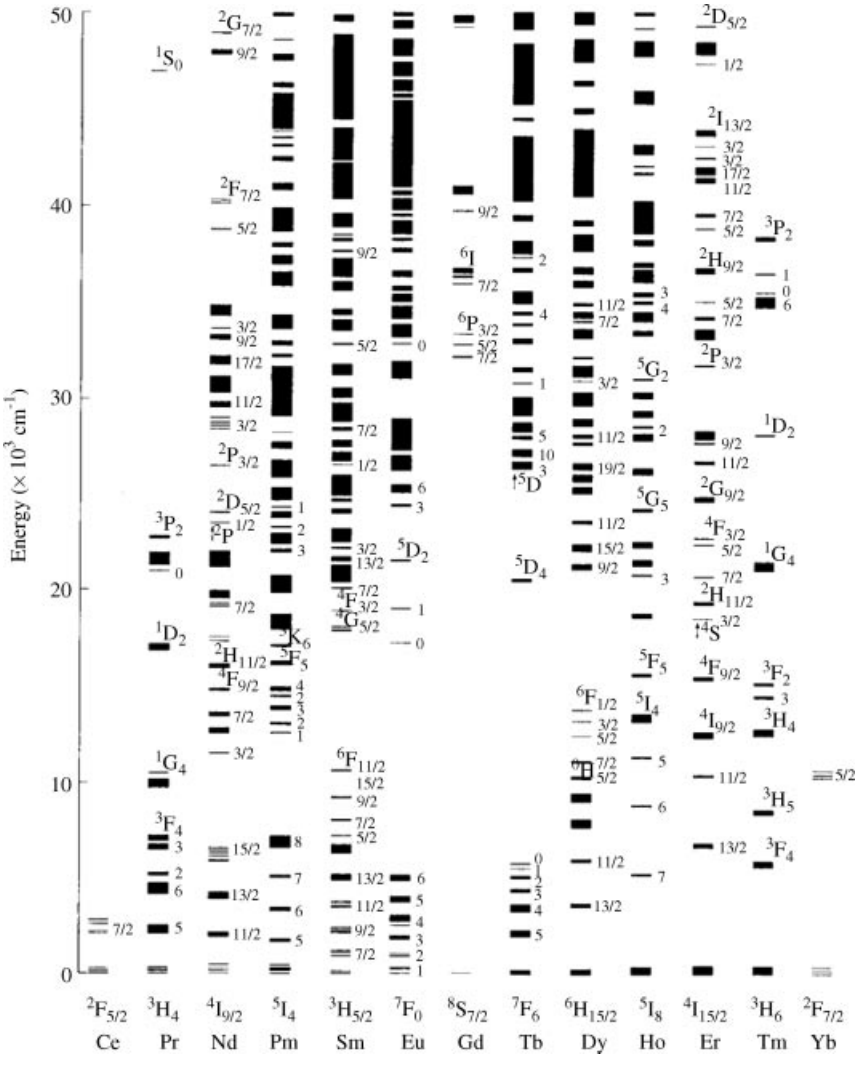


**Fig. 4.** Partial energy diagrams for $Ln^{III}$ ions doped into a low symmetry crystal, $LaF_3$. Reproduced with permission from Reference 34.

forbidden by both Laporte's and spin selection rules, whereas magnetic dipole transitions are allowed but are very weak. Henceforth, intensities of the 4f–4f transitions are rather weak, with molar absorption coefficients rarely larger than 10 and often smaller than $1\,M^{-1}cm^{-1}$. Some transitions are very sensitive to the metal-ion environment and are termed *hypersensitive* (or pseudo-quadrupolar) transitions; intensity enhancements may reach 200-fold. A list of these transitions is presented in Table 13 (33). They are very useful for analytical purposes.

2. Broader and more intense allowed 4f–5d transitions when a 4f electron is moved into an empty 5d orbital. These transitions are energetic and usually occur at $\lambda < 300\,nm$, with the exception of $Ce^{III}$ and sometimes $Tb^{III}$.

Table 12. **Number of Ligand-Field Sublevels Versus the Value of The Quantum Number *J***

| | | Integer *J* | | | | | | | | |
|---|---|---|---|---|---|---|---|---|---|---|
| Symmetry | Site symmetry | 0 | 1 | 2 | 3 | 4 | 5 | 6 | 7 | 8 |
| cubic | T, $T_d$, $T_h$, O, $O_h$ | 1 | 1 | 2 | 3 | 4 | 4 | 6 | 6 | 7 |
| hexagonal | $C_{3h}$, $D_{3h}$, $C_6$, $C_{6h}$, $C_{6v}$, $D_6$, $D_{6h}$ | 1 | 2 | 3 | 5 | 6 | 7 | 9 | 10 | 11 |
| trigonal | $C_3$, $S_6$ $C_{3v}$, $D_3$, $D_{3d}$ | | | | | | | | | |
| tetragonal | $C_4$, $S_4$, $C_{4h}$, $C_{4v}$, $D_4$, $D_{2d}$, $D_{4h}$ | 1 | 2 | 4 | 5 | 7 | 8 | 10 | 11 | 13 |
| low | $C_1$, $C_S$, $C_2$, $C_i$, $C_{2h}$, $C_{2v}$, $D_2$, $D_{2h}$ | 1 | 3 | 5 | 7 | 9 | 11 | 13 | 15 | 17 |
| Symmetry | Site symmetry | Half-integer *J* | | | | | | | | |
| | | 1/2 | 3/2 | 5/2 | 7/2 | 9/2 | 11/2 | 13/2 | 15/2 | 17/2 |
| cubic | T, $T_d$, $T_h$, O, $O_h$ | 1 | 1 | 2 | 3 | 3 | 4 | 5 | 6 | 6 |
| all others[a] | see above | 1 | 2 | 3 | 4 | 5 | 6 | 7 | 8 | 9 |

[a]All sublevels are doubly degenerate (Kramer's doublets).

3. Broad allowed charge-transfer transitions during which one electron is transferred from the metal ion to the bonded ligands (MLCT) or vice-versa (LMCT). MLCT transitions are very rarely identified in $Ln^{III}$ spectra, except for $Ce^{III}$, which can be readily oxidized into $Ce^{IV}$, the corresponding transition occurring up to 390 nm. There are also some reports of MLCT transitions for $Tb^{III}$ but at much higher energy and in the case of purely inorganic compounds. Ligand-to-metal charge transitions play an essential role in sensitizing the luminescence of phosphors used in modern lighting devices. As for 4f–5d transitions, LMCT transitions occur in the ultraviolet (uv) ($\lambda < 300$ nm), except for $Eu^{III}$ and $Yb^{III}$ for which they can extend up to 400 and 320 nm, respectively.

**7.2. Emission Spectra.** Barring $La^{III}$ and $Lu^{III}$, all $Ln^{III}$ ions are luminescent and their f–f emission lines cover the entire spectrum, from uv ($Gd^{III}$) to visible (eg, $Pr^{III}$, $Sm^{III}$, $Eu^{III}$, $Tb^{III}$, $Dy^{III}$, and $Tm^{III}$) and near-infrared (nir, eg, $Pr^{III}$, $Nd^{III}$, $Ho^{III}$, $Er^{III}$, and $Yb^{III}$) spectral ranges. Several ions are simultaneous visible and nir emitters (eg, $Sm^{III}$, $Eu^{III}$, $Er^{III}$, and $Tm^{III}$). Some ions are fluorescent ($\Delta S = 0$), others are phosphorescent ($\Delta S \neq 0$), and some are both. The 4f–4f emission lines are sharp because the electronic rearrangement consecutive to the promotion of an electron into a 4f orbital of higher energy does not perturb much the binding pattern in the molecules since 4f orbitals do not participate much in this binding (the covalency of $Ln^{III}$-ligand bonds is at most 5–7%). As a consequence, internuclear distances remain almost the same in the excited state, which generates narrow bands and very small Stokes shifts when the ions are excited directly. A different situation prevails in organic molecules for which excitation leads frequently to a lengthening of the chemical bonds, resulting in large Stokes shifts, because the coupling with vibrations is strong in broad emission bands. Typical emission lines observed in $Ln^{III}$ luminescence spectra are listed in Table 14 (35–37), together with other key photophysical parameters.

Table 13. **Identified Hypersensitive Transitions for $Ln^{III}$ Ions (wavelengths are approximate (33))**

| Ln | Transition | $\tilde{\nu}$, $cm^{-1}$ | $\lambda$, nm | Ln | Transition | $\tilde{\nu}$, $cm^{-1}$ | $\lambda$, nm |
|---|---|---|---|---|---|---|---|
| Pr | $^3F_2 \leftarrow {}^3H_4$ | 5200 | 1920 | Dy | $^6F_{11/2} \leftarrow {}^6H_{15/2}$ | 7700 | 1300 |
| Nd | $^4G_{7/2}, {}^2K_{13/2}, {}^2G_{9/2} \leftarrow {}^4I_{9/2}$ | 19 200 | 521 | | $^4G_{11/2}, {}^4I_{15/2} \leftarrow {}^6H_{15/2}$ | 23 400 | 427 |
| | $^4G_{5/2}, {}^2G_{7/2} \leftarrow {}^4I_{9/2_4}$ | 17 300 | 578 | Ho | $^3H_6 \leftarrow {}^5I_8$ | 27 700 | 361 |
| | $^2H_{9/2}, {}^4F_{5/2} \leftarrow {}^4I_{9/2}$ | 12 400 | 806 | | $^5G_6 \leftarrow {}^5I_8$ | 22 100 | 452 |
| Sm | $^4F_{1/2}, {}^4F_{3/2} \leftarrow {}^6H_{5/2}$ | 6400 | 1560 | Er | $^4G_{11/2} \leftarrow {}^4I_{15/2}$ | 26 400 | 379 |
| Eu | $^5D_2 \leftarrow {}^7F_0$ | 21 500 | 465 | | $^2H_{11/2} \leftarrow {}^4I_{15/2}$ | 19 200 | 521 |
| | $^5D_1 \leftarrow {}^7F_1$ | 18 700 | 535 | Tm | $^1G_4 \leftarrow {}^3H_6$ | 21 300 | 469 |
| | $^5D_0 \rightarrow {}^7F_2$ | 16 300 | 613 | | $^3H_4 \leftarrow {}^3H_6$ | 12 700 | 787 |
| Gd | $^6P_{5/2}, {}^6P_{7/2} \leftarrow {}^8S_{7/2}$ | 32 500 | 308 | | $^3F_4 \leftarrow {}^3H_6$ | 5900 | 1695 |
| Tb | [a] | | | | | | |

[a]None identified positively, but the $^5D_4 \rightarrow {}^7F_5$ transition sometimes display ligand-induced pseudo-hypersensitivity.

Table 14. **Ground (G), Main Emissive (E), and Final (F) States for Typical 4f–4f Emission Bands for $Ln^{III}$ Ions with Approximate Corresponding Wavelengths (λ), Energy Gap Between the Emissive State and the Highest Spin-Orbit Level of the Receiving State, and Radiative Lifetimes (35) (more nir lines are listed in Ref. 36)**

| Ln | G | E | F | λ, μm or nm[a] | Gap, $cm^{-1}$[a] | $\tau_{rad}$, ms[c] |
|---|---|---|---|---|---|---|
| Ce | $^2F_{5/2}$ | 5d | $^2F_{5/2}$ | tuneacle, 300–450 | – | – |
| Pr | $^3H_4$ | $^1D_2$ | $^3F_4$, $^1G_4$, $^3H_{4,5}$ | 1.0, 1.44, 600, 690 | 6940 | (0.05[c]–0.35) |
| | | $^3P_0$ | $^3H_{4\text{-}6}$ $^3F_{2\text{-}4}$ | 490, 545, 615 640,700, 725 | 3910 | (0.003[c]–0.02) |
| Nd | $^4I_{9/2}$ | $^4F_{3/2}$ | $^4I_{9/2\text{-}13/2}$ | 900, 1.06, 1.35 | 5400 | 0.42 (0.2–0.5) |
| Sm | $^6H_{5/2}$ | $^4G_{5/2}$ | $^6H_{5/2-15/2}$ | 560, 595, 640, 700, 775, 910 | 7400 | 6.26 (4.3–6.3) |
| | | $^4G_{5/2_4}$ | $^6F_{1/2\text{-}9/2}$ | 870, 887, 926, 1.01, 1.15 | | |
| | | $^4G_{5/2}$ | $^6H_{13/2}$ | 877 | | |
| Eu[d] | $^7F_0$ | $^5D_0$ | $^7F_{0\text{-}6}$ | 580, 590, 615, 650, 720, 750, 820 | 12 300 | 9.7 (1–11) |
| Gd | $^8S_{7/2}$ | $^6P_{7/2}$ | $^8S_{7/2}$ | 315 | 32 100 | 10.9 |
| Tb | $^7F_6$ | $^5D_4$ | $^7F_{6\text{-}0}$ | 490, 540, 580, 620 650, 660, 675 | 14 800 | 9.0 (1–9) |
| Dy | $^6H_{15/2}$ | $^4F_{9/2}$ | $^6H_{15/2\text{-}9/2}$ | 475, 570, 660, 750 | 7850 | 1.85 (0.15–1.9) |
| | | $^4I_{15/2}$ | $^6H_{15/2\text{-}9/2}$ | 455, 540, 615, 695 | 1000 | 3.22[c] |
| Ho | $^5I_8$ | $^5S_2$ | $^5I_{8,7}$ | 545, 750 | 3000 | 0.37 (0.51[c]) |
| | | $^5F_5$ | $^5I_8$ | 650 | 2200 | 0.8[c] |
| | | $^5F_5$ | $^5I_7$ | 965 | | |
| Er[e] | $^4I_{15/2}$ | $^4S_{3/2}$ | $^4I_{15/2,13/2}$ | 545, 850 | 3100 | 0.7[c] |
| | | $^4F_{9/2}$ | $^4I_{15/2}$ | 660 | 2850 | 0.6[c] |
| | | $^4I_{9/2_4}$ | $^4I_{15/2}$ | 810 | 2150 | 4.5[c] |
| | | $^4I_{13/2}$ | $^4I_{15/2}$ | 1.54 | 6500 | 0.66 (0.7–12) |
| Tm | $^3H_6$ | $^1D_2$ | $^3F_{4\text{-}2}$, $^3H_4$ | 450, 650, 740, 775 | 6650 | 0.09 |
| | | $^1G_4$ | $^3H_6$, $^3F_{4,5}$ | 470, 650, 770 | 6250 | 1.29 |
| | | $^3H_4$ | $^3H_6$ | 800 | 4300 | 3.6[c] |
| Yb | $^2F_{7/2}$ | $^2F_{5/2}$ | $^2F_{7/2}$ | 980 | 10 250 | 1.3 or 2.0[f] |

[a]Values for the aqua ions (37) otherwise stated.
[b]Ranges of observed lifetimes in all media, if available, between parentheses.
[c]Doped in $Y_2O_3$ or in $YLiF_4$ (Ho), or in $YAl_3(BO_3)_4$ (Dy).
[d]Luminescence from $^5D_1$, $^5D_2$, and $^5D_3$ is sometimes observed as well.
[e]Luminescence from four other states has also been observed: $^4D_{5/2}$, $^2P_{3/2}$, $^4G_{11/2}$, $^2H_{9/2}$.
[f]Complexes in solution: 0.7–1.3 ms; solid-state inorganic compounds: ≈2 ms.

## 8. Magnetic Properties of Lanthanide Ions

Effective magnetic moments for the free ions can be estimated within Russel–Saunders approximation with the following formula:

$$\mu_{\text{eff}} = g_J\sqrt{J(J+1)} \text{ with } g_J = \frac{J(J+1)+S(S+1)-L(L+1)}{2J(J+1)} \qquad (2)$$

$La^{III}$ ($4f^0$) and $Lu^{III}$ ($4f^{14}$) ions have $^1S_0$ ground levels and are diamagnetic. For the other ions, equation 2 gives satisfying results except for $Eu^{III}$ and, to a lesser extent, $Sm^{III}$, for which the first excited level is at low energy: $\approx 300\,cm^{-1}$ for the former, leading to a $^7F_1$ population of about 30% at room temperature, and $\approx 1000\,cm^{-1}$ for the latter. The orbital contribution is often important. Indeed, the most magnetic ion is not the one with the largest number of unpaired electrons ($Gd^{III}$) as exemplified in Table 15 and Figure 5.

The paramagnetism of $Ln^{III}$ ions finds application in the design of high coercivity magnets ($CoSm_5$ and $Fe_{14}Nd_2B$), magnetic resonance imaging (Gd complexes as contrast agents), shift reagents for interpreting nuclear magnetic resonance spectra, and magnetic refrigeration (38).

## 9. Toxicity

Whereas lanthanide metal vapors are highly toxic, lanthanide compounds are considered to be only slightly toxic in the Hodge–Sterner classification system and are safe when handled with ordinary care (39,40). The toxic effects of the lanthanides on humans have not been reported, but extensive tests of toxicity

Table 15. **Effective Magnetic Moments (B.M.) of Trivalent 4f Ions at 298 K**

| Ln | Conf. | $n^a$ | Ground state | First exc. state | $\Delta E$, $cm^{-1}$ | $g_J$ | $\mu_{calc}{}^b$ | $\mu_{calc}{}^c$ | $\mu_{exp}{}^d$ |
|---|---|---|---|---|---|---|---|---|---|
| Ce | $f^1$ | 1 | $^2F_{5/2}$ | $^2F_{7/2}$ | 2200 | 0.86 | 2.54 | 2.56 | 2.5–2.8 |
| Pr | $f^2$ | 2 | $^3H_4$ | $^3H_5$ | 2100 | 0.80 | 3.58 | 3.62 | 3.2–3.6 |
| Nd | $f^3$ | 3 | $^4I_{9/2}$ | $^4I_{11/2}$ | 1900 | 0.73 | 3.62 | 3.68 | 3.2–3.6 |
| Pm | $f^4$ | 4 | $^5I_4$ | $^5I_5$ | 1600 | 0.60 | 2.68 | 2.83 | n.a. |
| Sm | $f^5$ | 5 | $^6H_{5/2}$ | $^6H_{7/2}$ | 1000 | 0.29 | 0.85 | 1.60 | 1.3–1.5 |
| Eu | $f^6$ | 6 | $^7F_0$ | $^7F_1$ | 300 | [e] | 0 | 3.45 | 3.1–3.4 |
| Gd | $f^7$ | 7 | $^8S_{7/2}$ | $^6P_{7/2}$ | 32000 | 2.00 | 7.94 | 7.94 | 7.9–8.1 |
| Tb | $f^8$ | 6 | $^7F_6$ | $^7F_5$ | 2000 | 1.50 | 9.72 | 9.72 | 9.2–9.7 |
| Dy | $f^9$ | 5 | $^6H_{15/2}$ | $^6H_{13/2}$ | 3300 | 1.33 | 10.65 | 10.6 | 10.1–10.6 |
| Ho | $f^{10}$ | 4 | $^5I_8$ | $^5I_7$ | 5300 | 1.25 | 10.61 | 10.6 | 10.0–10.5 |
| Er | $f^{11}$ | 3 | $^4I_{15/2}$ | $^4I_{13/2}$ | 6500 | 1.20 | 9.58 | 9.6 | 9.2–9.6 |
| Tm | $f^{12}$ | 2 | $^3H_6$ | $^3F_4$ | 5800 | 1.17 | 7.56 | 7.6 | 7.0–7.3 |
| Yb | $f^{13}$ | 1 | $^2F_{7/2}$ | $^2F_{5/2}$ | 10000 | 1.14 | 4.54 | 4.5 | 4.3–4.6 |

[a] Number of unpaired electrons.
[b] Calculated according to equation 2.
[c] Exact calculation with van Vleck formula, taking into account the population of excited states.
[d] Ranges of experimentally observed values.
[e] Formula 2 yields an undetermined value; $g_J$ has been estimated to be $<5$.

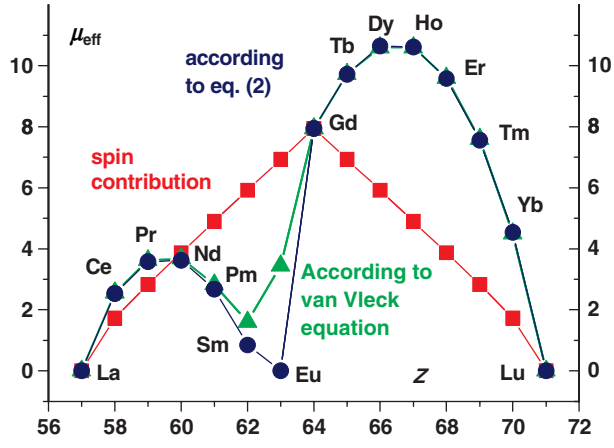


**Fig. 5.** Paramagnetic effective moments of $Ln^{III}$ ions (in Bohr magnetons).

have been conducted on animals. If the lanthanides are administered orally, then the toxicity is low. When rare-earth vapors or dusts are inhaled, they are somewhat more toxic although they are only slowly absorbed into the body. Dust and salts are very irritating to the eyes and mucus membranes and are moderately irritating to skin. Breathing the dust can cause lung embolism, and accumulated exposure damages the liver. Inhalation of rare-earth compound vapors or dust should therefore be avoided, and the skin should be washed thoroughly if it comes into contact with any dust or solution. If injected subcutaneously, then most of the injected material remains in place. The most detrimental reactions are obtained if lanthanides are introduced by means of intraperitoneal or intravenous injections. The symptoms of toxicity of the lanthanide elements include writhing, ataxia, difficult respiration, and sedation. Lanthanide ions can also interfere with calcium-containing proteins and calcium channels because $Ln^{III}$ ions can easily substitute $Ca^{II}$ ions. The $LD_{50}$ values for free $Ln^{III}$ ions for human beings are in the range 100–200 mg/Kg. Chelating agents, eg, citrate or EDTA, mask the toxic effects of lanthanide ions. The effect of atomic weight of lanthanides on lethality is difficult to assess, but the medium lanthanides seem to have a lesser toxicity than do light or heavy rare-earth elements. The toxicity of salts increases as follows: chloride < propionate < acetate < sulfate < nitrate. $LD_{50}$ values for lanthanide chlorides in mice are given in Table 16.

Table 16. **Lethal Doses $LD_{50}$ of Lanthanide Chlorides for Mice in Function of the Administration Route**

| $LnCl_3$ | Intraperitoneal $LD_{50}$ (mg/Kg) | Oral $LD_{50}$ (mg/Kg) | $LnCl_3$ | Intraperitoneal $LD_{50}$ (mg/Kg) | Oral $LD_{50}$ (mg/Kg) |
|---|---|---|---|---|---|
| La | 370 | n.a. | Tb | 550 | 5100 |
| Ce | 350 | n.a. | Dy | 585 | 7650 |
| Pr | 360 | 4500 | Ho | 585 | 200 |
| Nd | 600 | 5250 | Er | 535 | 6200 |
| Sm | 585 | <2000 | Tm | 485 | 6250 |
| Eu | 550 | 5000 | Yb | 395 | 6700 |
| Gd | 550 | <2000 | Lu | 315 | 6700 |

There is a delayed lethality after exposure to lanthanides; the death rate peaks between 48 and 96 h.

Lanthanides have no known biological role for human beings, although a 70-kg human contains 40 mg of cerium. However, lanthanides influence a wide range of plant processes by affecting cation transport and membrane structure (41). Some compounds inhibit the growth of organisms, whereas others seem to stimulate it; this is the case for tobacco plants and fish. These aspects are currently being investigated in more detail in light of the large usage of rare earths as fertilizers in China, the consequence of which is an increased Ln content in water (42).

## 10. Processing of Ores and Recycling

**10.1. Digestion of Rare-Earth Ores.** *Monazite.* The commercial process for monazite treatment is a digestion using caustic soda. The phosphate content of the ore is recovered as marketable trisodium phosphate and the rare earths as hydroxides. Typical industrial practice is to attack finely ground monazite with a 50% sodium hydroxide solution at 150°C or with a 70% sodium hydroxide solution at 180°C. The resulting mixed rare-earth and thorium hydroxide cake is dissolved in hydrochloric or nitric acid, then processed to remove thorium and other non–rare-earth elements, and finally treated to recover the individual rare earths.

*Bastnäsite.* The commercial 60% REO concentrate can be upgraded to 70% REO by leaching with hydrochloric acid followed by calcination. In the old Molycorp process, the flotation concentrate was heated in air at 620°C to remove $CO_2$ and oxidize cerium to the tetravalent state. The resulting solid was treated with 30% HCl to yield a marketable cerium concentrate containing 60–70% $CeO_2$ and to dissolve the other rare-earth elements. An alternative process consists in leaching the concentrate with hydrochloric acid so that the rare earths become partially dissolved, whereas a fraction combines with the fluoride from the ore. The mixed rare-earth fluoride residue is decomposed by using caustic soda; the resulting rare-earth hydroxides are then leached with HCl. Bastnäsite can also be treated with concentrated caustic soda at 200°C to form rare-earth hydroxides, which are dissolved in acid. A sulfuric acid treatment process consists in digesting the bastnäsite concentrate in concentrated sulfuric acid at 400°C and then in recovering the rare earths as water-soluble sulfates. Impurities such as iron are removed after neutralization.

**10.2. Loparite.** Two methods are used in Russia for loparite concentrate processing (43). The first one is a chlorination technique carried out using gaseous chlorine at 800°C in the presence of carbon. The volatile chlorides are subsequently separated from the calcium–sodium–rare-earth fused chlorides, and the resultant cake is dissolved in water. Alternatively, sulfuric acid digestion is carried out using 85% sulfuric acid at 150–200°C in the presence of ammonium sulfate. The ensuing product is leached with water, and while the double sulfates of the rare earths remain in the residue, titanium, tantalum, and niobium sulfates transfer into the solution. The residues are then converted into rare-earth carbonates.

**10.3. Separation Processes.** The product of ore digestion contains rare earths in essentially the same ratios as in the original ore, with few exceptions. This is because of the similar chemical properties of the various rare-earth elements. To give an idea of the amount of ore to be treated to obtain sometimes small quantities of pure rare earths, a scheme of the operations at Mountain Pass is presented in Figure 6. For instance, the production of 100 g of $Eu_2O_3$ requires the treatment of 1 metric ton of ore; however, this quantity is enough to manufacture the phosphors for about 300 energy-saving electric bulbs. More difficult to deal with is the simultaneous production of 200 g of radioactive thorium, which has to be disposed of according to strict regulations.

The various processes for separating individual rare earth from naturally occurring rare-earth mixtures essentially use small differences in acidity resulting from the decrease in ionic radius from lanthanum to lutetium. Acidity differences influence the solubility of salts, the hydrolysis of cations, and the formation of complex species so as to allow separation by fractional crystallization, fractional precipitation, ion exchange, and solvent extraction. Fractional precipitation and crystallization used in the twentieth century are now uneconomical.

The existence of tetravalent cerium and divalent europium species is useful because their chemical behavior is markedly different from that of the trivalent species. Cerium, the most abundant lanthanide, can be separated easily after oxidation of $Ce^{III}$ into $Ce^{IV}$. This simplifies the subsequent separation of the less abundant lanthanides. Oxidation occurs when bastnäsite is heated in air at 620°C or when the hydroxides are dried in air at 120–130°C. Once oxidized, $Ce^{IV}$ is separated from the trivalent lanthanides either by selective dissolution of trivalent species with dilute acid or by complete dissolution in concentrated acid followed by selective precipitation of ceric hydroxide [12014-56-1] or solvent extraction of $Ce^{IV}$ by tributylphosphate in a nitrate medium. In aqueous solution, oxidation of $Ce^{III}$ to $Ce^{IV}$ is carried out by treatment with hydrogen peroxide or sodium hypochlorite or by electrolysis. In aqueous solution, $Eu^{III}$ reduction into

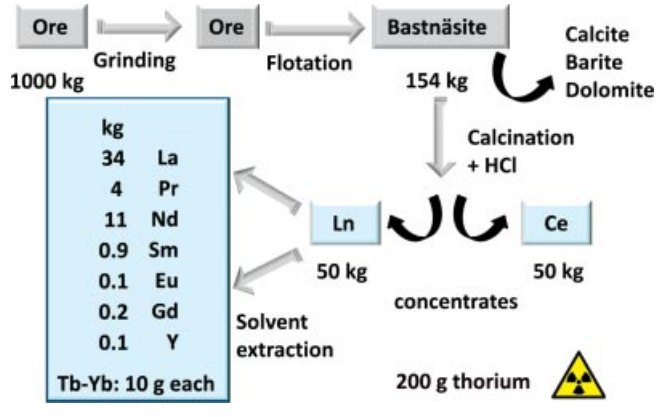


**Fig. 6.** Schematic representation of the treatment of bastnäsite ore at the Mountain Pass facility. For the sake of simplicity, it has been assumed that the REO content of the ore is 10% (actually around 8.9%) and the thorium content has been set at 200 ppm; for rare-earth composition, see Table 4.

$Eu^{II}$ is carried out by treatment with zinc. When reduced to the divalent state, europium exhibits chemical properties similar to those of alkaline-earth elements and can be selectively precipitated, as sulfate, for example. This process is highly selective and allows production of high purity europium.

*Ion Exchange.* Ion exchange has proved to be effective in the separation of high purity rare earths, but generally it involves the processing of very dilute aqueous solutions (44). In the 1950s, the commercial separation of the rare earths was dominated by ion-exchange methods, but technical and economic limitations have restricted its use in current industrial-scale separation processes. Mixed rare-earth cations in aqueous solution are strongly adsorbed by the organic cation-exchange resin. The rare earths are recovered by elution using a concentrated solution of a monovalent salt, for example, ammonium chloride. If a complexing agent exhibiting significantly different affinities for the various lanthanides is added to the eluent, then separation occurs. In practice, the process uses band-displacement techniques with aminopolycarboxylate eluents, such as EDTA and hydroxyethylene-diaminetriacetate (HEEDTA) among others. Small amounts of lanthanides continue to be separated by ion exchange for specific grades, such as >99.9999% purity. Some new developments have been proposed, but the main limitation of the ion-exchange process is the low solubility of RE aminopolycarboxylates in aqueous solution. Ion exchange was largely replaced by liquid–liquid extraction during the 1960s for this reason.

*Liquid–Liquid Extraction.* Liquid–liquid extraction for rare-earth separation was proposed by Fischer in 1937 (45): Extraction of REE with simple alcohols, ethers, or ketones gave separation factors of up to 1.5. The selectivity of the distribution of two rare-earth elements, RE1 and RE2, between two nonmiscible liquid phases is given by the ratio of the distribution coefficients, $D_1$ and $D_2$:

$$D_1 = \frac{[\mathrm{RE1}]_{\mathrm{or}}}{[\mathrm{RE1}]_{\mathrm{aq}}} \quad D_2 = \frac{[\mathrm{RE2}]_{\mathrm{or}}}{[\mathrm{RE2}]_{\mathrm{aq}}} \quad F = \frac{D_1}{D_2} \tag{3}$$

The subscripts "or" and "aq" stand for the organic and aqueous phases, respectively, and $F$ is the separation factor. For two neighboring trivalent rare earths, $F$ is usually small; thus, for an effective separation, many single separation operations have to be repeated, batch wise or continuously. A fully continuous liquid–liquid extraction process in countercurrent flow enables separation into two groups of REE to be achieved. Thus, the separation of $n$ REE requires $n+1$ countercurrent separations carried out using a column or mixer–settler arrangement. A schematic flow diagram of a countercurrent flow extraction plant for the continuous separation of two REE or two groups of REE is shown in Figure 7. The mixture to be separated is fed into an intermediate stage of the contactor operating in countercurrent flow. The solvent becomes preferentially charged with the REE that form the most stable complex, whereas the REE that forms the less stable complex remains in the aqueous phase. The flow extract is further washed by the scrubbing aqueous solution to remove traces of the less stable REE complex. The pure extract is then subjected to backextraction to recover a high purity aqueous solution. The solvent is then recycled. Solvent systems generally consist of at least the following components:

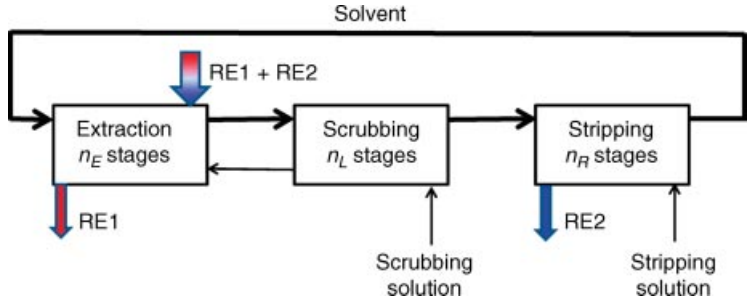


**Fig. 7.** Schematic representation of a counterflow liquid–liquid extraction process.

extractant, diluent, inorganic salts or acids, and water. The relative concentrations of these components have to be carefully optimized to achieve efficient separation. A key factor to success is the choice of the appropriate extractant. Many extractants, acidic, basic, or neutral, may be used.

*Acidic Extractants.* They react with REE according to a cation-exchange reaction:

$$Ln^{3+}(aq) + 3\,HL(org) \rightarrow [LnL](org) + 3\,H^{+}(aq) \qquad (4)$$

The extent of extraction or backextraction is therefore governed by the pH of the aqueous phase. Extraction by carboxylic acids is carried out in a neutral or weakly acidic medium. The most widely used carboxylic acid is $(R_1)(R_2)(CH_3)C\text{-}COOH$, where $R_1$ and $R_2$ are alkyl chains. Trade names are Versatic 10 [CAS 26896-20-8] (Shell Chemicals, Houston, Tex) or Neodecanoic acid (Exxon Chemicals, Irving, Tex), which contain a total of 10 carbon atoms. Naphthenic acids are also used. Carboxylic acids can be used either in chloride or in nitrate media. Many commercial acidic organophosphorus extractants are available: dialkylphosphoric acids, $(RO)_2PO(OH)$; alkyl alkylphosphonic acids, $R(RO)PO(OH)$; and dialkylphosphinic acids, $R_2PO(OH)$. The most popular alkyl chains are 2-ethylhexyl (Albright & Wilson, Victoria, Australia; Bayer, Leverkusen, Germany; Daihachi Chemicals Co. Ltd., Osaka shi, Japan) and 2,4,4-trimethylpentyl (Cytec Industries, Inc., Woodland Park, NJ). 2-Ethylhexyl phosphonic acid 2-ethylhexyl ester (HEHEHP) is widely used by rare-earth processors. The efficiency of extraction by the organophosphorus acids decreases with decreasing acidity constant, specifically in the order phosphoric > phosphonic > phosphinic derivatives, whereas the selectivity within the lanthanide series is adversely affected.

*Basic Extractants.* Long-chain quaternary ammonium salts, $R_3NCH_3{}^{+}X^{-}$, in which R is a C8–C12 alkyl group and X is nitrate or thiocyanate, are effectively used for REE separations. The extractant reacts with REE according to an anion-exchange reaction:

$$Ln^{3+}(aq) + 3\,X^{-}(aq) + R_3MeN^{+}X^{-}(org) \rightarrow [LnX_4{}^{-}R_3MeN^{+}](org) \qquad (5)$$

The extent of extraction or backextraction is governed by the concentration of $X^{-}$ in the aqueous phase; the distribution coefficients and selectivity depend on the

anion. In nitrate solutions, the distribution coefficient decreases as the atomic number of the REE increases, whereas in thiocyanate solutions, the distribution coefficient roughly increases as the atomic number of the REE increases. The position of yttrium in the lanthanide series is not the same in nitrate and thiocyanate solutions. A combination of extraction by carboxylic acids and by ammonium salts is used for production of high purity yttrium.

*Neutral Extractants.* Many neutral organophosphorus extractants are available: phosphate esters, phosphonate esters, phosphinate esters, and phosphine oxides. The most common neutral extractant is tributylphosphate (TBP), which reacts with REE according to a solvation mechanism:

$$Ln^{3+}(aq) + 3\,NO_3^-(aq) + 3\,TBP(org) \rightarrow [Ln(NO_3)_3(TBP)_3](org) \qquad (6)$$

The extent of extraction can be increased by a salting-out effect. The selectivity of TBP is very poor compared with HDEHP, and this extractant is therefore useful only for light rare-earth separation; organic phase loadings higher than 100-g REO per liter can easily be achieved.

*Equipment.* The preferred extraction technique in the rare-earth industry uses mixer–settlers. This technology is suitable for the relatively small flow rates in the REE refineries and the large number of stages required for the production of high purity REE. Some difficult separations require batteries of more than 100 stages.

**10.4. Production.** *Salts and Oxides.* The final step in the chemical processing of rare earths depends on the intended use of the products. Rare-earth oxides are obtained by firing at 900°C hydroxides, carbonates, or oxalates precipitated from aqueous solutions. Rare-earth chlorides are produced by crystallization of aqueous chloride solutions, whereas fluorides are precipitated with hydrofluoric acid.

*Metals and Alloys.* The preparation of metals has been outlined in the Basic Properties of Lanthanide Elements section. Alloys for magnets, eg, SmCo5, are produced by reducing a mixture of samarium and cobalt oxides with calcium at about 1000°C, leading to a mixture of SmCo5 and CaO, which is removed subsequently by leaching. The $Nd_2Fe_{14}B$ magnets additionally contain aluminum (0.2–0.4%), niobium (0.5–1%), and dysprosium (0.8–1.2%), as well as sometimes small amounts of cobalt, copper, and/or gadolinium. The required amounts of Nd, Fe, and B are introduced into an induction furnace, and an alloy is formed ("Neo" alloy). The ingots are then broken down by hydrogen decrepitation and jet milled in a nitrogen/argon atmosphere into a 3-μm powder; magnets are pressed from this powder.

**10.5. Economical Aspects.** Rare-earth technology is one of the most fascinating and challenging industries in the world. The recent geopolitical turmoil has drawn the attention of the scientific community and of the general public to the specificity of this market. The industry is regularly shaken by big swings in supply and demand, appearance of new applications, entrance of new competitors, and sometimes new raw materials. The rare-earth market can be considered for some segments as a specialty business, whereas for others, it exhibits the characteristics of a commodity business. Up to the early 1980s, rare earths were used mostly in low technology applications (lighter flints,

Table 17. **Average Prices in the United States of Selected Lanthanide Oxides in 2008–2012**[a]

| Ln oxide | 2008 | 2009 | 2010 | 2011 | 2012 | January 2013 |
|---|---|---|---|---|---|---|
| La | 8 | 6 | 23 | 100 | 23 | 10 |
| Ce | 4 | 4 | 21 | 100 | 24 | 11 |
| Pr | 27 | 15 | 46 | 195 | 115 | 82.5 |
| Nd | 27 | 15 | 47 | 230 | 115 | 77.5 |
| Eu | 475 | 465 | 550 | 2850 | 2400 | 1550 |
| Tb | 650 | 350 | 530 | 2300 | 1950 | 1250 |
| Dy | 110 | 100 | 225 | 1450 | 1000 | 615 |
| Y | 15 | 14 | 26 | 140 | 90 | 35 |

[a]Values are in U.S. dollars per kg, FOB China. Prices in China are about 30% cheaper. Note that prices depend on quality and volumes.

fluid-cracking catalysts, and metallurgy), but now they are widely used in high technology applications: phosphors for lamps and displays, lasers and amplifiers for telecommunications, high performance magnets, rechargeable batteries, automotive catalysts, superconducting ceramics, computers and smartphones, security inks, counterfeiting tags, and medical imaging and analyses to name but a few. In fact, the market is split into two distinct segments: applications that require nonseparated rare earths (glasses, fluid-cracking catalysts, metallurgy, rechargeable batteries, polishing powders, and fertilizers) and applications for which separated, and often very pure, rare earths are needed such as catalysts for polymer synthesis or water treatment, magnets, phosphors, optics, electronics, luminescent tags, and biosciences.

The consumption patterns of rare earths vary considerably between major economic areas and evolve rapidly. Until recently, Japanese, European, and American markets were dominated by high value applications while the Chinese market was more concentrated on nonseparated rare earths. This, however, is changing fast.

The prices for selected lanthanide oxides over the time period 2008–2012 are gathered in Table 17. They clearly reflect the big upsurge consecutive to the fears for shortage in 2009–2010. But the start of operations by Molycorp (Mountain Pass, Calif.) and Lynas (Mount Weld, Australia/Malaysia for separation) in 2012 as well as a slowdown of the world economy put pressure on REO prices that seemed to be heading back toward the 2010 levels in January 2013. Operations in Baotou were even stopped for 4 months to try to stabilize prices.

**10.6. Recycling.** In many existing industrial applications, rare earths are used as additives at a relatively low mass ratio. In practice, it is difficult to recycle them economically, and as a consequence, rare-earth recycling is still not performed on large scale. But the situation is changing with new regulations in the handling and disposal of industrial and domestic residues and because prices of mined rare earths have been increasing substantially lately (but see the preceding section). One advantage of recycling over mine production is that industrial products do not contain thorium, and this may be a significant factor helping recycling to develop. Companies are recycling rare earths either from in-plant produced scrap during the manufacturing or from industrial products that reached their end of life. Although details of rare-earth recycling are often

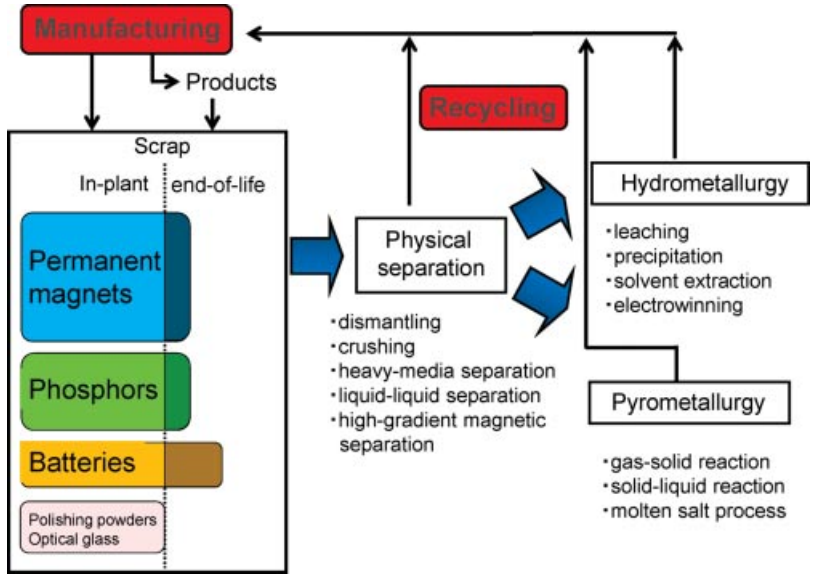


**Fig. 8.** Overview of recycling processes for in-plant and end-of-life rare-earth products (with approximate proportions given by the shadowed sections on the right-hand part of the figure).

proprietary, a significant number of academic papers have been recently published. Figure 8 gives an overview on the main recycling processes currently in use; for updated reviews, see References 46 and 47. Few data from China are available, but it seems that recycling operations are also underway.

*Magnets.* In current practice, rare-earth recovery started in the magnet industry. Lanthanide-rich residues are produced during the fabrication of Nd- and Sm-containing magnets. Processes have therefore been developed using classic separation techniques that led to the recovery of up to 90–95% of these scraps. In the case of NdFeB, the residues are oxidized by calcination and dissolved in acid; after separation of iron and boron, the neodymium-containing solution is treated by solvent extraction techniques (hydrometallurgy), and the lanthanide is transformed into oxide before being reduced to produce the metal. End-of-life products are somewhat more difficult to recycle because magnets are often tightly mounted and difficult to separate from other materials (particularly in electronics such as smartphones and hard-disk drives (HDDs) where the quantity of magnet is very small and the magnet difficult to dismantle) and because of coatings (eg, nickel coating to avoid corrosion) or mixture of different magnets. Methods currently used include hydrometallurgy and pyrometallurgy and magnets are recovered from air-conditioner compressor, laundry and dishwasher machines, from larger motors and compressors, as well as from hard-disk drives (although they only contain 0.6 wt % of rare earths). Such operations are pursued by Santoku Corporation (Kobe, Japan) and Umicore (Brussels, Belgium) since 2012, while Solvay-Rhodia (Paris, France) is also working on such a project.

*Phosphors.* Recycling of rare-earth phosphors as such can only be made in some special cases, namely, when the phosphor material can be scraped out of

the tubing. This is possible with straight fluorescent tubes (although mercury poses a problem) but not with winded energy-saving bulbs. In the latter case, lamps have to be crashed and the phosphor separated from the glass powder and then dissolved and separated by solvent extraction methods. Solvay-Rhodia reopened two of its extraction facilities in La Rochelle (France) for this purpose in 2012. Since 2012 as well, BluBox Trading A.G. (Birrwil, Switzerland) is proposing a fully automated, container-style module for the recycling of lamp and display phosphors.

*Metal Hydride Batteries.* The negative electrode of these rechargeable batteries contains an $LnM_5$ hydrogen-absorbing alloy where Ln = La or "mischmetall" and M = Ni or Co. On average, such batteries contain 24 wt % of Ln, 68 wt % of Ni, and 8 wt % of Co. Although a few recycling processes have been designed during the past 15 years by several research groups to recover both rare earths and the transition metals, the first recycling facilities only started operations in September 2011 in Belgium (Umicore, Hoboken plant; in collaboration with Solvay-Rhodia for extraction/separation) and March 2013 at the Japan Metals & Chemicals Company plant (Tokyo, Japan) on behalf of automobile maker Honda in Japan.

*Polishing Powders and Catalysts.* Here again, complete recovering schemes have been worked out, but because the main lanthanide involved is cerium, which is rather cheap, it seems that they have not yet been transposed into the practical world.

## 11. End Uses of Rare Earths

The end uses of lanthanides depend on the countries; eg, there are large differences between the United States, Europe, and Asia. The market is not easy to follow in light of the small amounts of REO used per year (the total amount would fit in a single cargo shipment!) and in light of the multitude of products into which rare earths are provided. With respect to the world's metal production in 2010, rare earths represented only 0.01% in weight (steel: 90%; technology metals: 1%). Estimated data for rare-earth applications in 2010 are displayed in Figure 9. Catalysts, glass additives, and polishing powders, as well as

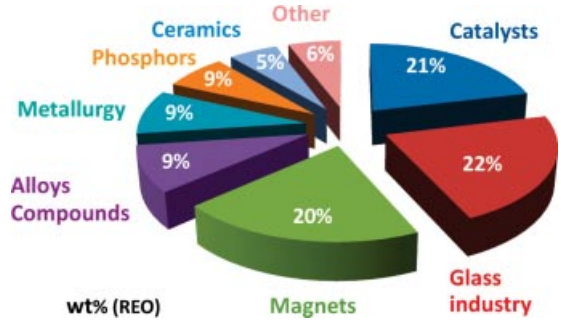


**Fig. 9.** Uses of rare earths with respect to main applications. Data from U.S. Geological Survey Report 2011-5094 and Mineral commodity summaries 2012. Percentages expressed with respect to REO.

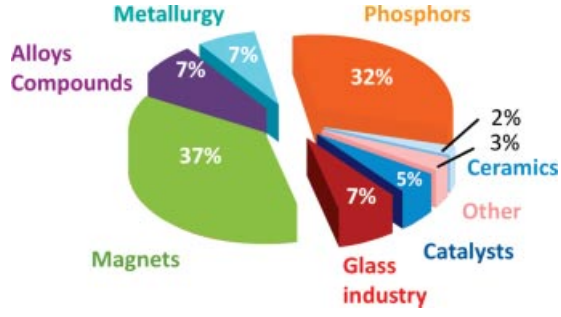


**Fig. 10.** Relative value of rare-earth-containing end products. Data from V. Nicoletopoulos, Rare Earths Worldwide: An Industry and Policy Analysis (June 2011).

magnets, represent almost two thirds of the tonnage used. However, magnets and phosphors are the leaders with more than two thirds of the commercial value (Fig. 10). Usages with respect to individual elements are displayed in Figure 11; here again, there is a large dissymmetry in that La, Ce, Nd, Pr, and Y represent 97 wt % of all rare earths used in end products. Major end uses for lanthanides and their compounds are listed in Table 18. The detailed presentation of rare-earth applications in the subsequent sections follows the order of economic importance.

**11.1. Magnetic Properties and Magnets.** Rare-earth metals have exceptional magnetic properties. At a low temperature, magneto-crystalline anisotropy constants are 10–100 times higher than for other elements and absolute saturation magnetization is much higher than in iron, for example. However, magnetic ordering occurs only at low temperatures, as the internal character of the 4f orbital induces weak couplings for direct interactions between neighboring atoms as well as for long-range exchange via conduction electrons. Thus, rare-earth metals are diamagnetic or paramagnetic at room temperature; the highest Curie temperature $T_c$ is 292.7 K for gadolinium (Table 7), below which

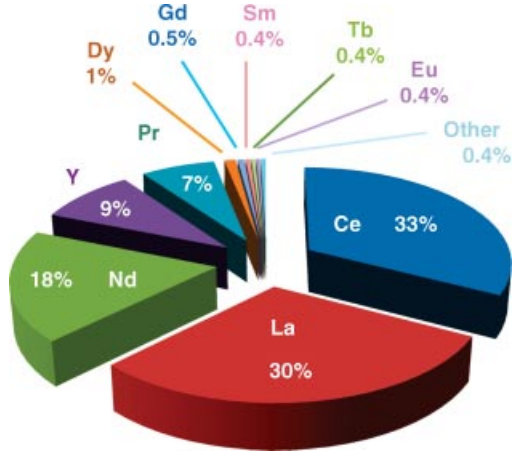


**Fig. 11.** Uses of rare earths with respect to individual elements. Same sources as in Figure 9.

Table 18. **Major End Uses for Lanthanide Elements and Compounds**

| Element | End uses | Element | End uses |
|---|---|---|---|
| La | metal alloys ("mischmetall"), rechargeable batteries | Dy | permanent magnets (hybrid engines) |
| Ce | metal alloys ("mischmetall"), automotive catalysts cracking catalysts, polishing powders | Er | laser and waveguide amplifiers (telecommunications) upconverting phosphors (security inks, counterfeiting tags, bioanalyses) |
| Pr | permanent magnets | Ho | glass coloring lasers |
| Nd | permanent magnets (HDD, headphones, smartphones, wind turbines), catalysts, lasers | Tm | medical x-ray units |
| Sm | permanent magnets | Lu | catalysts (petroleum refining) |
| Eu | red phosphors (lighting, displays) | Yb | lasers, steel alloys |
| Gd | permanent magnets, medical imaging, refrigeration | Sc | scandium-aluminum alloys for aerospace components |
| Tb | green phosphors (lighting, displays), permanent magnets | Y | metal alloys, matrices for phosphors |

it becomes ferromagnetic. However, Curie temperatures can be increased to commercially interesting levels by alloying lanthanide metals with elements having higher ordering temperatures, such as the transition metals, iron, cobalt, or nickel. The first high performing magnetic materials to be industrialized were samarium–cobalt magnets, mainly $SmCo_5$. These magnets displayed intrinsic coercivity >20 kOe and $T_C$ >700°C. This enabled the miniaturization of many electronic devices, such as stepping motors and headphones for the famous Walkman (Sony, New York, NY) introduced in 1979 (fabrication of the tape edition was discontinued in 2010). The growth of applications was, however, limited by the relative scarcity and high cost of samarium and cobalt. This limitation was removed by the discovery of the 2.5 times more powerful neodymium–iron–boron magnets in 1984 (48). Magnets based on the $Nd_2Fe_{14}B$ structure are produced as 100% dense sintered products using classic powdered metallurgy processes and as bonded materials in epoxy or nylon. Applications range from HDDs and magnetic resonance imaging (MRI) to innumerable automotive and electronic ones. The current and future demand for Nd permanent magnets is primarily determined by three major applications: electric motors for hybrid and electric vehicles, wind turbines, and hard disks, to which can be added magnets for magnetic resonance, both in research and in medical imaging. The coercivity of these magnets can be enhanced (particularly at a high temperature) by adding a small amount of dysprosium.

*Electric and Hybrid Vehicles.* The growth of this market is still steady, despite relatively high prices. For instance, the legendary first hybrid vehicle, the Toyota Prius (Toyota, Aichi Prefecture, Japan), requires 1 kg of neodymium for its electric motors. Currently, electric and hybrid cars use Ni/Ln hydride batteries so that this market stimulates La and Ce markets as well.

*Wind Turbines.* In 2010, installed wind power capacities were estimated to be 175 GW with China representing a 20% share but almost 50% of the new installations. Several technologies are in use for wind turbines, but the one taking advantage of Nd-magnets seems to be the best because it does not require a gearbox so that it is the technology of choice for off-shore turbines because maintenance is easier. There are, however, some debates as to whether this is the best "green" technique because one turbine needs about 550 kg of Nd (with associated environmental nuisances for its production). In addition, rising prices for Nd have to be considered: Some manufacturers are ready to switch to iron-only magnets if the price of Nd reaches an uneconomical level.

*Hard Disk Drives, Data Storage, and Electronic Components.* The Japanese firm Shin-Etsu Chemical Company (Tokyo, Japan) estimates that 30% of the Nd-magnets are used in hard disk drives for personal computers (PCs) and laptop computers and 10% in optical and acoustic applications (including buzzers for smartphones, for instance). Although the number of PCs, laptops, tablets, and smartphones produced will certainly increase in the next decades, substitution of HDDs with the solid-state drive (SSD) technology will probably lead to a relatively modest increase in the use of Nd with respect to this market. Rare-earth transition-metal alloys are also applied in magneto-optic recording, in which the magnetic (high coercivity field and low $T_c$) and optical (high value of the Kerr rotation angle) properties of (Gd, Tb)(Co, Fe) amorphous alloys are used to obtain high recording densities (20 Mbits/cm$^2$) in laser

erasable–rewritable compact disks. Supercomputers contain Gd-based bubble memory substrates.

*Scientific and Medical Applications.* Nd-magnets are the core of nuclear magnetic spectrometers and scanners that use large permanent magnets. No substitution is in sight, and the market should develop steadily.

**11.2. Phosphors and Scintillators.** All next-generation, energy-saving lighting and display technologies require the use of rare earths as light-converting materials (phosphors) providing high energy efficiency and high color rendering. Implied elements are europium (trivalent: red, 610 nm; divalent: blue, 450 nm) and terbium (green, 550 nm) as emitters, cerium as sensitizer for terbium, and yttrium, lanthanum, and gadolinium as matrices. The major applications are fluorescent tubes, compact fluorescent lamps (CFLs), and plasma and liquid crystal (LCD) displays, which have replaced the old cathode-ray tube (CRT) displays. Other devices include light-emitting diodes (LEDs), electroluminescent foils, and possibly, organic light-emitting diodes (OLEDs), although currently the latter use iridium and platinum complexes as luminescent emitters. In light of the growing ban on the sale of incandescent bulbs (European Union, the United States, Canada, and Australia), the market has a good future, especially that of LEDs, which represent only <5% market share in 2010 and are assumed to sustain a growth rate of 20–30% in the next few years. Hundreds of millions of smartphones are also produced currently, and their total number is estimated to grow to 2 billion in 2012, but altogether this represents only about 400 tons of nine different rare earths (Y, La, Ce, Pr, Sm, Eu, Gd, Tb, and Dy).

Some phosphors are used as temperature sensors because the emitted luminescence intensity is sensitive to this parameter; examples include YAG:$Ln^{III}$ phosphors (YAG is yttrium aluminum garnet, $Y_3Al_5O_{12}$) with Ln = Sm or Dy (range: 300–1700 K) (49).

Some long-persistence phosphors, that is, light emission from which is slow and lasts long after excitation, are found in watch dials, emergency signs and markings, and toys and gadgets. A typical compounds is $Ca_2Si_5N_8:Eu^{II},Tm^{III}$. Other compounds such as $Y_2SiO_5:Eu^{III}$ allow optical storage by persistent hole burning (50). Security inks, counterfeiting tags, and ammunition markers are often made from rare-earth phosphors. This represents a small but showcase market for lanthanides. A particular category of such phosphors includes the up-converting phosphors, often provided under the form of nanoparticles: UCNPs, which contain ytterbium as sensitizers and erbium (green and red) or thulium (blue) as emitters. UCNPs and long-persistent phosphors are currently being tested in medical imaging (51).

Finally, the principal applications of scintillators are for the measurement of uv radiations in the range 200–220 nm or x-rays in medical imaging and the detection of radioactivity (medical imaging and security checks). Typical ions for these applications are trivalent cerium and divalent europium (52).

**11.3. Metallurgy, Alloys, and Compounds.** *Metallurgy.* Applications in this field are old and rely on the strong affinity of rare-earth metals for oxygen and sulfur. Small amounts of "mischmetall" act as trap for these elements, usually detrimental to the properties of steel or cast iron. This results in better resistance to high temperature oxidation and thermomechanical properties of several metals and alloys, for instance, by hardening stainless steel or

producing a malleable iron. The addition of 3–4% cerium to magnesium alloys in addition to 0.2–0.6% zirconium results in a grain refinement and allows a sound casting of complex shapes. The resistance of aluminum to corrosion can also been improved by addition of cerium.

*Alloys.* Another old application is the pyrophoric alloys in flint ignition devices for lighters and torches. But the "mischmetall" is also used as a minor component in the casting of steel, which improves the stability of the end product. The addition of Y, La, or Ce to heat-resistant alloys also increases their performances. Scandium is the most potent strengthener of aluminum, and Sc-Al alloys (0.1–0.5 wt% Sc) are suitable for small aerospace (essentially in military aviation) and weapon components. It also appears in high performance materials for high level sport competition (bicycles and baseball bats).

*Energy-Related Materials.* Nickel-lanthanide hydride (Ni-LnH) batteries are found in electric (EV) and hybrid electric (HEV) vehicles and in portable appliances (smartphones and cameras, for instance). In fact these batteries contain "mischmetall" and a blend of nickel and cobalt. Almost 60% of these batteries equip EVs and HEVs. The demand for them will therefore be dominated by the growth of the HEV market. However, some growth predictions for the Ni-LnH market made in 2008 were based on the basis that the Toyota Prius batteries contain 10–15 kg of rare earths; a later estimate (2011) put this number at only about 3 kg. In addition, substitution by lithium batteries is being foreseen, but lithium is also a rare element and fire problems may slow a large dissemination of these batteries despite their definite advantages over Ni-LnH batteries. Solid oxide fuel cells (SOFCs) represent the most promising technology for fuel cells. They contain yttrium in the electrolyte and "mischmetall" in the electrodes.

*Water Treatment.* A mixed rare-earth chloride solution marketed under the brand name sorbX100 by Molycorp (Greenwood Village, Colo.) leads to rapid and stable precipitation of phosphates in municipal and industrial wastewater facilities.

**11.4. Glass Industry.** *Cerium Oxide.* Rare earths are widely used in the glass industry, particularly cerium. For instance, discoloration of glass is obtained through oxidation of iron from its deep-blue divalent form to the pale-yellow trivalent one by tetravalent cerium. Furthermore, cerium oxide is the best polishing agent for glass because of its natural hardness, a consequence of its compact fluorite structure and a chemical reaction at the silica–cerium oxide interface. Purity and morphology of the polishing powders made from cerium oxide can be adapted to the polishing quality required. Cerium oxide is also a uv-blocking material that is used in sunglasses and could potentially be fitted onto dye-sensitized solar cells to prevent photodegradation of the dye.

*Colored Glasses, Ceramics, and Plastics.* Praseodymium (green), neodymium (purple), and erbium (pink) are used to color glasses and ceramics. Zircon (ZrSiO4) doped by tetravalent praseodymium is the strongest and most stable yellow pigment for ceramics with high firing temperatures. Pigments for the coloration of plastics and paints are based on the optical properties of cerium sulfide derivatives and their nontoxicity. These are an alternative to heavy-metal-based pigments like cadmium sulfoselenides. Because of the doping by alkali or alkaline earths, it has been possible to stabilize a range of colors from orange to bright red and maroon in the form of $Ce_2S_3$. These pigments feature

high brightness and tinting strength, a good stability in the application media (polymers such as polypropylene, acrylonitrile butadiene styrene, and polycarbonate), and a strong resistance to weathering and uv, which makes cerium sulfide-based pigments good candidates for a wide range of applications (53). Other optical applications involve $Ce^{IV}$ as an antibrowning agent for glass or lanthanum as a component (40 wt %) in high refractive index borate glasses for microscope, telescope, and camera lenses.

*Lasers.* In light of their numerous and well-defined electronic levels, lanthanides ions are well suited as active materials for solid-state lasers emitting in the uv, visible, or nir. The only limitation is the transparency of the matrix (54). The lasing materials are often single crystals that have to be carefully grown to avoid defects. A good thermal conductivity is also required to evacuate the heat: Yields of lasing are low, so that a great amount of energy is transformed into heat. One of the most widely used lasers is YAG:$Nd^{III}$ (see the Phosphors and Scintillators section), which produces a line at 1.06 μm, the frequency of which can easily be doubled (532 nm, green; eg, laser pointers for slide presentations), tripled (355 nm, blue), or quadrupled (266 nm, uv), leading to multiline lasers for excitation of luminescence spectra. To enhance its yield, $Cr^{III}$ or $Ce^{III}$ are often introduced in the garnet as sensitizer. The YAG garnet can be doped by several other lanthanide ions, giving rise to lasers emitting at 1.03 μm (Yb), 1.93–2.04 μm (Tm), 2.1 μm (Ho + Tm), and 2.94 μm (Er). Low power lasers, particularly those emitting at long wavelengths, are used in several medical applications: eye surgery, skin treatment, and dentistry, or for monitoring the sugar content in blood. High power YAG:Nd lasers (or arrays of them) are used in manufacturing and even for atomic fusion (eg, the 500-TW laser systems at the National Ignition Facility, Lawrence Livermore Laboratory, Livermore, Calif.).

Optical fibers are now ubiquitous in telecommunications, but despite their excellent transparency, the signals get too much attenuated after 50 or 100 km and need amplification. Because $Er^{III}$ is emitting in the main telecommunication window (C band, 1.5 μm), glasses doped with this ion are ideal waveguide amplifiers (38,54). Other rare-earth lasing materials feature tunable uv and visible lasers, self-frequency doublers (38), and lasers for optical refrigeration (55).

**11.5. Catalysts.** Rare earths are mentioned as active elements in a large number of catalytic reactions, and several areas have reached industrial level. The oldest one is the structural and chemical stabilization of zeolites for oil cracking applications (fluidized cracking catalysts [FCCs]), where the addition of several percent of lanthanides (mainly lanthanum and/or cerium) allows the catalyst to remain acidic, which is essential for the conversion of high molecular weight molecules into lighter species, especially in the very aggressive conditions of the petroleum industry (56). Cerium oxide is also the catalyst provided in self-cleaning domestic ovens.

Another important application for cerium oxide is automotive postcombustion catalysts. First, it is a major component of the three-way catalysts (TWCs) used in all modern gasoline cars. TWCs lower the level of pollutant emissions from the engine through selective reduction of nitrogen oxides ($NO_x$) and simultaneous oxidation of carbon monoxide and hydrocarbons. As cerium can be either trivalent or tetravalent, redox properties of $CeO_2$ can make it an oxygen buffer stabilizing the composition of exhaust gases and allowing oxidation of CO and

hydrocarbons even when the medium is globally reducing. The catalyst is made of 100–3000 ppm of precious metal (Pd, Rh, or Pt) dispersed on a mixture of alumina and cerium oxide (20 wt%). In addition to its major role in the control of redox conditions of the medium, cerium oxide is highly refractory and allows alumina to keep its surface thermally stable at the elevated temperatures seen by the catalytic muffler (>1000°C). Finally, it also permits a good, thermally stable dispersion of the metallic particles, the actual catalyst, preventing them from sintering, which would make them inactive. The development of cerium–zirconium mixed oxides has led to improved performances in terms of oxygen buffering capacity and thermal stability. Based on the industrial development of highly efficient chemical methods, special grades of cerium–zirconium oxides, remaining active at higher temperatures, have been developed for automotive catalysts.

Diesel engines enjoy growing popularity because of their fuel efficiency (30% more mileage than a gasoline engine) and drivability. However, they face major challenges in controlling particulate matter (PM) and $NO_x$ emissions. The most efficient way to reduce particulate matter emissions is to filter the exhaust gases. However, because the filter becomes blocked as the soot particles accumulate, the technological challenge has been to find a way to eliminate these particles. The best solution is to burn them to regenerate the filter. Rhodia (now Solvay-Rhodia) has developed an efficient filter/catalyst system based on cerium oxide (Eolys®; Solvay-Rhodia). The fuelborne catalyst facilitates filter regeneration by significantly lowering the temperature at which the soot burns, from >600°C to around 350°C, and by increasing the kinetics of combustion, typically 2–3 minutes instead of 20–23 minutes for the competing technologies. The performance of Eolys® technology is independent of the engine-out $NO_x$/PM ratio and does not increase $NO_2$ emissions. The catalyst is added to the fuel from a 1.7-L tank, which allows for a service interval of 250,000 km for an average passenger car and a similar filter service life. Toxicological studies have demonstrated the nonhazardous nature of Eolys®. No secondary gaseous or particulate emissions occur when used in conjunction with a particulate filter, and >99.9% of emitted particles are eliminated. The product is compatible with the majority of plastics and elastomers used in the manufacture of fuel tanks, fuel pumps, and fuel lines. In 2012, more than 4 million vehicles were equipped with this system; retrofitting to light-, medium- and heavy-duty vehicles is easy. The market growth for this product is very high.

Among the other catalytic applications of rare-earth compounds, one can mention the use of divalent samarium halides in organic synthesis (57). But another area for rare-earth usage is having a very rapid growth: the use of neodymium salts as a diene polymerization catalyst (58). For example, with respect to polybutadiene, the use of neodymium carboxylates allows for getting high cis-polybutadiene content and a very good control of the molecular weight distribution of the polymer. Other advantages of the use of rare-earth salts compared with transition elements are high polymerization temperatures, reducing the cooling stage of the polymer, and substituting toxic aromatic solvents by aliphatic ones. This leads to a significant industrial development of the use of neodymium salts for rubber manufacturing. Among other tested materials are lanthanide triflates for enantioselective synthesis of pharmaceuticals (59) as

well as amidinates, guanidinates (60), and borohydride (61) complexes for ring-opening polymerization.

**11.6. Ceramics.** Chemical and structural properties of the rare earths are also used in the ceramics industry. Minute additions of rare-earth oxides stabilize tetragonal or cubic forms of zirconia. Among them, yttrium oxide (1–10 mol %) is the best compromise. Stabilized forms of zirconia are used in sensors (for their high ionic conductivity), cutting tools (for their good thermomechanical properties), or imitation jewelry (when the cubic form is fully stabilized, for $Y_2O_3$ content above 7 mol %). Most of the high temperature (H-$T_C$) superconductors discovered in the late 1980s involve yttrium, eg $YBa_2Cu_3O_7$. These ceramics that conduct electricity without resistance have still a limited use because they do not work at room temperature, but they can be made into power cables (although of limited length), magnets (in particle accelerators or for magnetic levitation trains), and switching stations, for example. The Superamic (Solvay-Rhodia) ceramics enter in electronic equipment as microwave filters, high performance capacitors, or oxygen sensors. In particular, barium titanate doped with $Nd^{III}$ has a dielectric constant that does not change over a large temperature range. An overview of ceramics applications is given in Table 19.

**11.7. Other Uses.** Gadolinium has the highest cross section for thermal neutrons ever known, 46,000 barns per atom (1 barn $= 10^{-28}\,m^2$), and is used extensively in nuclear reactors as a component fuel or in control rods, where it acts as a consumable poison, a trap for neutrons in the reactor. This metal and some of its compounds such as $Gd_5(Si_{1-x}Ge_x)_4$ display huge magnetocaloric effects that make them potential candidates for magnetic refrigeration; although a demonstrator has been built, practical applications are, however, not yet at hand (62).

*Defense Applications.* Military uses of rare earths span the range of applications of these elements. Rare earths are indispensable for night vision, guiding systems, laser weapons, motorization, aircraft electric generators, and light alloys for jet turbines as well as for stabilizing rocket nose cones, jamming and sonar devices, antimissile systems, range finders, satellite power and telecommunication systems, and radar systems. Some of these aspects are vital; armies are closely following the rare-earth markets and stockpiling some of the most critical metals and compounds.

*Agriculture.* There are two main uses of rare earths in agriculture. The first one has been essentially pursued by China since the early 1970s and consists of applying a mixture of lanthanide salts or complexes as fertilizers (63). There are three main products: *Changle-Yishizu* based on nitrates and

Table 19. **Main Rare-Earth Applications in Ceramics**

| Application | RE used |
|---|---|
| capacitors, semiconductors components for LCDs and electronics | La, Ce, Pr, Nd |
| stabilizers for ceramics | Y, Ce |
| H-$T_C$ ceramics | Y |
| pigments for ceramics | Y, Pr, Nd |
| refractory materials | Y, Ce |
| dental ceramics | Ce |
| garnets for laser materials | Y |

containing about 32 wt % equivalent REO (19.9% La, 4.7% Ce, 1.9% Pr, 5.4% Nd, 0.3% Sm, <0.1% Eu, and Gd); *Nongle*, which contains lanthanide chlorides (38 wt % equiv. REO); and *MAR* comprising a mixture of $Ln^{III}$ complexes (Ln = La, Ce, Pr, and Nd) with 17 different amino acids (64). These mixtures further contain several other elements essential to plant growth and are sometimes applied along with herbicides/pesticides or vitamin C. Application methods are either spraying (eg, wheat, mushrooms, bananas, and tea) or blending/immersing seeds (eg, maize, potatoes, and alfalfa). Initially reported increases in crop or fruit production reached up to 20–30% (50% for tobacco), but these numbers have to be taken with caution because the experimental conditions or control experiments were often not described (41). Currently, it seems that increases of about 10–15% are reasonably established (64), although some studies conclude to much smaller effects, if at all. An estimated 16–29 million ha of cultures were treated with rare earths in China in 1995; taking a range of 150–200 g REO/ha, this would correspond to a consumption of 2400–5800 tons of REO per year. We also note that phosphate-based fertilizers in common use in agriculture contain sizeable amounts of rare earths (65). The second usage relies on wavelength-converting materials, mainly simple europium salts and complexes, as additives to agriculture plastics. Detrimental uv light is absorbed and transformed into red light, which has good conversion efficiency in photosynthesis (66). Here also, increases in crop yields of about 10% are reported. This result is sizeable, but the dark side of this application is the use of costly and relatively rare europium. Currently, it is difficult to estimate the future of such a market.

In 2006, the European Union has banned the use of antibiotics in animal food. This has stirred interest for the development of alternative methods and substances to promote growth. Because there is a link between plant and animal growth, rare-earth compounds have been tested to this end, particularly in Germany and Switzerland, following Chinese experiments. In most studies, dietary application of rare earths did not influence the health of animals, meat quality, or the safety of the products while improving growth performances of pigs, poultry, sheep, goats, calves, horses, fish, and prawns. The reported increase in body weight is around 20% (40% for sheep and goats) and increases in egg or milk production range between 15 and 20%, but there are contradictory reports; in particular, fattening of bulls with diets containing rare-earth citrates did not produce positive results (67). The main rare-earth-containing compounds used in these diets are chlorides, nitrates, or complexes with ascorbate or citrate, and the dosage is usually 100–200 mg/kg of feed. Regarding cost, it was estimated in 2006 that the application of rare earths to animal diets would cost about one Swiss franc per 100 kg of food (63).

*Medical Applications.* Applications in bioanalyses and bioimaging are gaining momentum (68), especially since the advantage of luminescent immunoassays over radioactive ones was recognized; these optical analyses do not require much lanthanide (typically 1 μg per analysis), and despite that they rely on rarer and costly lanthanides (Sm, Eu, Tb, Dy, Er, Tm, and Yb), they do not have much impact on the raw rare-earth market. Gadolinium complexes play the role of contrast agents in nuclear magnetic medical imaging, and the consumption is relatively important because about 2 g of Gd are required per image. More than 26 million such analyses are carried out each year in the

United States alone, with increased applications in chest, vascular, breast, and cardiac imaging, translating in the need for 52 tons of gadolinium per year in this country alone. Despite large improvements in the spectrometers that work now at a much higher field and the advent of multimodal techniques, the need for gadolinium contrast agents will remain steady (69), especially now that software packages for the analysis of cardiovascular magnetic resonance images have been available since 2013; the market is expected to grow 5% per year.

*Photovoltaics.* This field is growing fast, but because of some bottlenecks leading to relatively poor conversion efficiencies, lanthanide compounds are being examined for their ability as wavelength-converting materials. Indeed, semiconductors (silicon, gallium arsenide, and titanium dioxide) have the best conversion efficiency at a wavelength $\lambda[\text{nm}] = 1240/E_B$, where $E_B$ is the bandgap in eV. For crystalline Si, this translates to $\approx$1.1 μm. Therefore, the idea is to use downconversion (production of two 1.1-$\mu$m photons from one uv/blue photon) or upconversion (addition of two IR photons to produce one 1.1-μm photon) to boost the conversion yields of solar cells. The field is still in its infancy, and even in laboratory tests, the bettering adds up to only 1–2 absolute percent (51). Nevertheless, intense research is currently being conducted toward this goal and might lead to concrete applications. Similarly, lanthanides may be used as photocatalysts for either water splitting or degradation of organic substance during water purification (70).

## BIBLIOGRAPHY

"Rare-Earth Metals" in *ECT* 1st ed., Vol. 11, pp. 503–521, by H. E. Kremers, Lindsay Chemical Co.; "Rare-Earth Elements" in *ECT* 2nd ed., Vol. 17, pp. 143–168, by W. L. Silvernail and N. J. Goetzinger, American Potash & Chemical Corp.; in *ECT* 3rd ed., Vol. 19, pp. 833–854, by F. H. Spedding, Iowa State University, "Lanthanides", in *ECT* 4th ed., vol. 14, pp.1091–1115, by Jean-Lovis Sabot and Patrick Maestro, Rhône - Poulenc Recherches; "Lanthanides", in *ECT* (online), posting date: December 4, 2000, by Jean-Lovis Sabot and Patrick Maestro, Rhône - Poulenc Recherches; in *ECT* 5th edition, Vol. 14, pp. 630–654, by A. Leveque and J. L. Sabot, Rhodia Rare Earths and P. Maestro, Rhodia SA; in *ECT* (online), posting date July 13, 2001, by A. Leveque and J. L. Sabot, Rhodia Rare Earths and P. Maestro, Rhodia SA.

## CITED PUBLICATIONS

1. S. M. McLennan and S. R. Taylor, in D. A. Atwood, ed., *The Rare Earth Elements: Fundamental and Applications*, Wiley, Chichester, U.K., 2012, pp. 1–19.
2. P. Thyssen and K. Binnemans, in K. A. Gschneidner Jr., J.-C. G. Bünzli, and V. K. Pecharsky, eds., *Handbook on the Physics and Chemistry of Rare Earths*, Vol. 41, Elsevier Science B.V., Amsterdam, 2011.
3. K. A. Gschneidner Jr. and A. H. Daane, in K. A. Gschneidner Jr., and L. Eyring, eds., *Handbook on the Physics and Chemistry of Rare Earths*, Vol. 11, Elsevier Science B.V., Amsterdam, 1998.
4. N. B. Mikheev, *Inorg. Chim. Acta* **94**, 241 (1984).
5. L. J. Nugent and co-workers, *J. Phys. Chem.* **77**, 1528 (1973).

6. E. N. Rizkalla and G. R. Choppin, in K. A. Gschneidner Jr. and L. Eyring, eds., *Handbook on the Physics and Chemistry of Rare Earths*, Vol. 15, Elsevier Science Publ. B.V., Amsterdam, 1991.
7. V. Haase, H. K. Kugler, M. Lehl-Thalinger, and U. Trobisch-Raussendorf, in *Gmelin's Handbook of Inorganic Chemistry "Sc,Y,La-Lu,"* Vol. B7, Springer Verlag, Berlin, Germany, 1979, pp. 1–23.
8. Y. Suzuki and co-workers, *J. Less-Common Met.* **126**, 351 (1986).
9. R. D. Shannon, *Acta Cryst*. **A32**, 751 (1976).
10. G. Meyer, in D. A. Atwood, ed., *The Rare Earth Elements: Fundamental and Applications*, Wiley, Chichester, U.K., 2012, pp. 161–173.
11. F. Nief, in K. A. Gschneidner Jr., J.-C. G. Bünzli, and V. K. Pecharsky, eds., *Handbook on the Physics and Chemistry of Rare Earths*, Vol. 40, Elsevier Science B.V., Amsterdam, 2010.
12. C. Huang and Z. Bian, in C. Huang, ed., *Rare Earth Coordination Chemistry, Fundamentals and Applications*, Wiley, Singapore, 2010, pp. 1–40.
13. V. S. Sastri, J.-C. G. Bünzli, V. R. Rao, G. V. S. Rayudu, and J. R. Perumareddi, *Modern Aspects of Rare Earths and Complexes*, Elsevier Science B.V., Amsterdam, 2003.
14. L. C. Thompson, Complexes, in K. A. Gschneidner Jr. and L. Eyring, eds., *Handbook on the Physics and Chemistry of Rare Earths*, Vol. 3, North Holland Publ. Co., Amsterdam, 1979.
15. H. C. Aspinall and M. R. Tillotson, *Polyhedron*, **13**, 3229 (1994).
16. G. W. Rabe, J. Riede, and A. Schier, *J. Chem. Soc. Chem. Commun.* 577 (1995).
17. D. M. Barnhart and co-workers, *Inorg. Chem.* **34**, 4862 (1995).
18. R. D. Rogers and E. J. Voss, *Inorg. Chim. Acta* **133**, 181 (1987).
19. R. D. Rogers and A. N. Rollins, *J. Chem. Cryst.* **24**, 531 (1994).
20. M. R. Spirlet and co-workers, *Inorg. Chem.* **23**, 4278 (1984).
21. E. Moret and co-workers, *J. Less-Common Met.* **171**, 273 (1991).
22. J. Y. Hu, Q. Shen, and Z. S. Jin, *Chin. Sci. Bull.* **35**, 1090 (1990).
23. C. Piguet and co-workers, *Inorg. Chem.* **32**, 4139 (1993).
24. J.-C. G. Bünzli and co-workers, *J. Inorg. Nucl. Chem.* **42**, 1307 (1980).
25. J.-C. G. Bünzli and co-workers, *Inorg. Chim. Acta* **54**, L43 (1981).
26. B. Eriksson, L. O. Larsson and L. Niinistö, *J. Chem. Soc. Chem. Commun.* 616 (1978).
27. J.-C. G. Bünzli and co-workers, *Inorg. Chem.* **21**, 808 (1982).
28. J.-C. G. Bünzli, B. Klein, and D. Wessner, *Inorg. Chim. Acta* **44**, L147 (1980).
29. M. D. Lind, B. Lee and J. L. Hoard, *J. Am. Chem. Soc.* **87**, 1611 (1965).
30. A. E. Martell and R. M. Smith, *Critical Stability Constants*, Plenum Press, New York, 1974.
31. W. P. Cacheris, S. K. Nickle, and A. D. Sherry, *Inorg. Chem.* **26**, 958 (1987).
32. L. Helm and A. E. Merbach, *Chem. Rev.* **105**, 1923 (2005).
33. J.-C. G. Bünzli and S. V. Eliseeva, in O. S. Wolfbeis and M. Hof, eds., *Springer Series on Fluorescence. Lanthanide Luminescence: Photophysical, Analytical and Biological Aspects*, Vol. 7, Springer Verlag, Berlin, Germany, 2011.
34. G. K. Liu, in G. K. Liu and B. Jacquier, eds., *Spectroscopic Properties of Rare Earths in Optical Materials*, Vol. 83, Springer Verlag, Berlin, Germany, 2005, pp. 1–94.
35. J.-C. G. Bünzli and S. V. Eliseeva, in V. W.-W. Yam, ed., *Comprehensive Inorganic Chemistry II*, Vol. 8, Elsevier B.V., Amsterdam, 2013, in press.
36. S. Comby and J.-C. G. Bünzli, in K. A. Gschneidner Jr., J.-C. G. Bünzli, and V. K. Pecharsky, eds., *Handbook on the Physics and Chemistry of Rare Earths*, Vol. 37, Elsevier Science B.V., Amsterdam, 2007.

37. W. T. Carnall, in K. A. Gschneidner Jr., and L. Eyring, eds., *Handbook on the Physics and Chemistry of Rare Earths*, Vol. 3, North Holland Publ. Co., Amsterdam, 1979.
38. S. V. Eliseeva and J.-C. G. Bünzli, *New J. Chem.* **35**, 1165 (2011).
39. R. A. Bulman, in A. Sigel and H. Sigel, eds., *Metal Ions in Biological Systems*, Vol. 40, Marcel Dekker Inc., New York, 2003.
40. T. J. Haley, in K. A. Gschneidner Jr., and L. Eyring, eds., *Handbook on the Physics and Chemistry of Rare Earths*, Vol. 4, North Holland Publ. Co., Amsterdam, 1979.
41. P. H. Brown, A. H. Rathjen, R. D. Graham and D. E. Tribe, K. A. Gschneidner Jr., and L. Eyring, eds., *Handbook on the Physics and Chemistry of Rare Earths*, Vol. 13, Elsevier Science Publ. B.V., Amsterdam, 1990.
42. M. P. Ippolito and co-workers, *Arch. Environ. Contamin. Toxicol.* **58**, 42 (2012).
43. V. D. Kosynkin and co-workers, *J. Alloy. Compd.* **192**, 118 (1993).
44. J. E. Powell, F. H. Spedding, and D. B. James, *J. Chem. Educ.* **37**, 629 (1960).
45. W. Fischer, W. Dietz, and O. Jübermann, *Naturwissenschaften* **25**, 348 (1937).
46. M. Tanaka, T. Oki, K. Koyama, H. Narita, and T. Oishi, R.in J.-C. G. Bünzli, and V. K. Pecharsky, eds., *Handbook on the Physics and Chemistry of Rare Earths*, Vol. 43, Elsevier Science, B.V., Amsterdam, 2013.
47. K. Binnemans and co-workers, *J. Clean. Prod.*, **22**, (2013).
48. M. Sagawa and co-workers, *J. Appl. Phys.* **55**, 2083 (1984).
49. L. P. Goss, A. A. Smith, and M. E. Post, *Rev. Sci. Instr.* **60**, 3702 (1989).
50. Y. C. Sun, in G. K. Liu and B. Jacquier, eds., *Spectroscopic Properties of Rare Earths in Optical Materials*, Springer Verlag, Berlin, Germany, 2005, pp. 379–429.
51. J.-C. G. Bünzli and S. V. Eliseeva, *Chem. Sci.* **4**, 1939, (2013).
52. H. A. Hoppe, *Angew. Chem. Int. Ed.* **48**, 3572 (2009).
53. J.-N. Berte, in H. M. Smith, ed., *High Performance Pigments*, Wiley-VCH Verlag GmbH & Co. KGaA, Weinheim, Germany, 2001, pp. 27–40.
54. R. Moncorge, in G. K. Liu and B. Jacquier, eds., *Spectroscopic Properties of Rare Earths in Optical Materials*, Vol. 83, Springer Verlag, Berlin, Germany, 2005, pp. 320–378.
55. M. P. Hehlen, in I. R. Epstein and M. Sheik-Bahae, eds., *Optical Refrigeration: Science and Applications of Laser Cooling of Solids*, Wiley-VCH, Mannheim, 2009, pp. 33–74.
56. D. N. Wallace, in K. A. Gschneidner Jr., ed., *Industrial Applications of Rare Earth Elements*, American Chemical Society, Washington, D.C., 1981, pp. 101–116.
57. H. B. Kagan and co-workers, *J. Alloys Compd.* **192**, 191 (1993).
58. D. E. Bergbreiter, L. B. Chen, and R. Chandran, *Macromolecules* **18**, 1055 (1985).
59. K. Shen and co-workers, *Chem. Sci.* **3**, 327 (2012).
60. F. T. Edelmann, *Chem. Soc. Rev.* **41**, 7657 (2012).
61. S. M. Guillaume, L. Maron, and P. W. Roesky, in J.-C. G. Bünzli, and V. K. Pecharsky, eds., *Handbook on the Physics and Chemistry of Rare Earths*, Vol. 44, Elsevier Science, B.V., Amsterdam, 2013, in press.
62. K. A. Gschneidner Jr., V. K. Pecharsky, and A. O. Pecharsky, *Rep. Prog. Phys.* **68**, 1479 (2005).
63. K. Redling, PhD. Dissertation, Ludwig-Maximilians-Universität München, 2006.
64. X. Pang, D. Li, and A. Peng, *J. Soils Sedim.* **1**, 124 (2001).
65. C. Turra, E. A. N. Fernandes, and M. A. Bacchi, *J. Envir. Chem. Ecotoxicol.* **3**, 86 (2011).
66. C. Edser, *Plastics, Additives & Compounding* **4**, 20 (2002).
67. A. Schwabe and co-workers, *Arch. Anim. Nutrit.* **65**, 55 (2011).

68. J.-C. G. Bünzli, *Chem. Rev.* **110**, 2729 (2010).
69. A. M. Blamire, *Brit. J. Radiol.* **81**, 601 (2008).
70. A. S. Weber, A. M. Grady, and R. T. Koodali, *Catal. Sci. Technol.* **2**, 683 (2012).

## GENERAL REFERENCES

S. Cotton, *Lanthanide and Actinide Chemistry*, Wiley, Chichester, U.K., 2006.
D. A. Atwood, *The Rare Earth Elements: Fundamentals and Applications*, Wiley, Chichester, U.K., 2013.
J.-C. G. Bünzli and V. K., Pecharsky, eds., *Handbook on the Physics and Chemistry of Rare Earths*, Elsevier Science, B.V., Amsterdam, 44 volumes published to date.
B.T. Kilbourn, *Cerium: A Guide to its Role in Chemical Technology*, Molycorp Inc., White Plains, N.Y., 1993.
B. T. Kilbourn, *A Lanthanide Lanthanology, Part I (A-N), Part II (M-Z)*, Molycorp Inc., White Plains, N.Y., 1993.
*Gmelin Handbuch der Anorganische Chemie, System Nr. 39, "Y,Sc,La-Lu"*, 8th ed., Springer Verlag, Berlin, Germany, 1977.

JEAN-CLAUDE G. BÜNZLI
Korea University & Swiss Federal Institute of Technology